39p

DETERMINATION OF THE HEMISPHERICAL SPECTRAL EMITTANCE OF CARBON, GRAPHITE, ZIRCONIA, AND ABLATION MATERIAL CHARS FROM 0.37 TO 0.72 MICRON AND 3,000° F TO 6,000° F

By R. Gale Wilson [1963] ref.

NASA Langley Research Center
Langley Station, Hampton, Va.

For ~~Presentation~~ presentation at the ~~Fifth~~ 5th Symposium on Thermal Radiation of Solids,

San Francisco, ~~California~~
March 4-6, 1964

DETERMINATION OF THE HEMISPHERICAL SPECTRAL EMITTANCE OF CARBON, GRAPHITE, ZIRCONIA, AND ABLATION MATERIAL CHARS FROM 0.37 TO 0.72 MICRON AND 3,000° F TO 6,000° F*

By R. Gale Wilson**

NASA Langley Research Center

ABSTRACT

16610

The initial results of the application of special optical techniques to emittance and reflectance studies of reentry heat-shield ablation material chars at high temperatures to determine their effectiveness in radiation cooling are presented. An Arthur D. Little-Strong Arc Imaging Furnace and Image Pyrometer have been equipped with selected filters and detectors suitable for providing measurements of hemispherical spectral reflectance on opaque materials at wavelengths extending throughout the visible spectrum and into the near ultraviolet. Reflectance and emittance were determined for carbon, graphite, zirconia, and a particular ablation material char at wavelengths from 0.37 micron to 0.72 micron and for temperatures from 3,000° F to 6,000° F. Surface-roughness properties of the materials were measured with a Carl Zeiss Light-Section Microscope and statistically treated. The performance of the equipment and reliability of the data are discussed.

AUTHOR

INTRODUCTION

At velocities associated with reentry into the earth's atmosphere from earth-orbital or outer-space missions, flight vehicles experience aerodynamic heating which produces surface temperatures above the melting or vaporization temperatures of conventional structural materials. Thermal protection systems have been devised in which ablating materials are used effectively to protect the load-carrying structures of these vehicles. Charring ablation materials have been shown to be particularly effective for use in thermal protection systems (see refs. 1 and 2) because of their capability to reradiate a significant portion of the heat absorbed. However, a detailed understanding of the complex

---

*The information presented herein is taken from a thesis which will be offered in partial fulfillment of the requirements for the degree Master of Arts, The College of William and Mary, Williamsburg, Virginia.

**Aerospace Technologist.

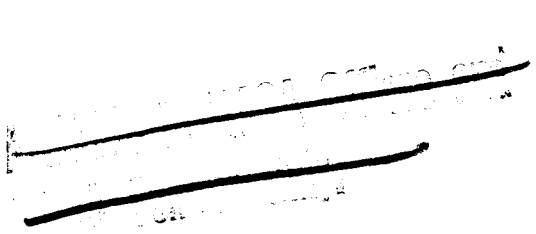

behavior of charring ablators requires extensive analytical and experimental studies, including a determination of the emittance and absorptance characteristics of the chars at performance temperatures.

The object of the present investigation was to apply special optical techniques to emittance and reflectance studies on certain ceramic and carbonaceous materials, including a particular ablation material char, over a range of wavelengths and temperatures. The experimental apparatus used for reflectance measurement consisted of an Arthur D. Little-Strong Arc Imaging Furnace and an image pyrometer designed for operation in conjunction with the arc imaging furnace. Several filter-detector combinations were selected for a range of wavelengths covering the visible and extending into the near ultraviolet spectrum. Hemispherical spectral emittance (absorptance) values were calculated from the reflectance measurements. Suitable attenuation of arc irradiation of the sample provided for measurements from about 3,000° F to 6,000° F. Surface roughness of the materials was measured optically and was statistically treated to qualify the emittance data with regard to the surface properties of the materials. The performance of the equipment and reliability of the data are discussed.

DESCRIPTION OF METHODS AND APPARATUS

Apparatus for Measurement of Reflectance and Temperature

The dependence of emittance on temperature and nonexistence of general theoretical relationships for predicting emittance as a function of temperature make it impossible to calculate or accurately predict high-temperature radiation properties from low-temperature data. Although measurement of either total or spectral emittance at high temperatures does not differ in principle from that at low temperatures, there are problems associated with extending standard techniques of measurement to very high temperatures. In using the black-body-comparison method, it is difficult not only to obtain the required high temperatures but also to measure radiation emitted by the sample only, excluding that emitted by hot furnace walls or reflected by the sample. Of equal difficulty is the construction of black-body cavities operational at very high temperatures which are known to be the same as those of the sample. The practicability of thermoelectric temperature measurements at high temperatures is limited by the low melting points of thermocouple materials and the susceptibility of thermocouple materials to contamination by other materials.

For the present investigation an arc imaging furnace with an integrated image pyrometer was utilized to heat the material samples and to determine the spectral emittance and temperature relationships at high temperatures. This method circumvents the problems noted above. The arc imaging furnace is described by Glaser in reference 3, and the image pyrometer and its principles of operation are described by Comstock in reference 4. Briefly, the arc imaging furnace, shown schematically in figure 1, consists of a double-ellipsoidal-mirror optical system with two 21-inch-diameter mirrors located coaxially and facing each other at a

a distance of about 7 feet. An electric arc radiation source is located at the minor focal point of one mirror and its image is formed at the minor focal point of the other mirror. At the minor focal plane of the re-imaging mirror there is a sample support motorized for movement in three mutually perpendicular directions to provide for precise optical alignment of the sample with respect to the mirrors and arc.

The image pyrometer, illustrated schematically in figure 2, is an instrument designed for operation between the two ellipsoidal mirrors of the arc imaging furnace at the midplane where the major focal points of the mirrors coincide. The two coincident images of arc and sample formed in the midplane are scanned by rotating light pipes whose signals are fed through an optical filter to a photomultiplier. The output of the photomultiplier is then amplified and fed into an oscillographic recorder, producing radiation profiles across the images of the arc and the sample. The image pyrometer incorporates a rapidly rotating chopper which provides for scanning of the sample in rapid succession with the arc radiation incident on the sample and with the arc radiation briefly obstructed from the sample. From the radiation profile of the arc and of the sample with and without incident arc radiation, along with separate measurements on a standard reflectance sample and a standard temperature source, the spectral reflectance and temperature of the sample at every point across its irradiated surface can be calculated.

Apparatus for Measurement of Surface Roughness

Inasmuch as the emittance of any material varies with surface conditions, it was considered desirable in the present investigation to define the mocro-geometric properties of the material surfaces on which temperature and emittance were determined. A Carl Zeiss Light-Section Microscope was chosen for making the measurements because it permits measurements on soft materials without destroying or altering the surface. One arrangement for use of the light-section method to measure surface roughness is described in reference 5. In the Carl Zeiss instrument a microscope is used for the optical measurement of the surface-profile image produced by the light-section method, as shown schematically in figure 3(a). The incandescent lamp Q illuminates the slit S, which, by means of the objective O_1, is reproduced on the surface being studied as a thin band of light. This band of light closely follows and illuminates the surface along its contour, and a profile image of the surface may be observed and/or photographed through a microscope whose objective O_2 has the same magnification as O_1. Illumination and observation directions form a 90° angle with each other and 45° angles with the surface being examined. A reticle R, visible in the eyepiece O, may be shifted within the field of view by means of a micrometer drum. Because the light band meets the surface at an angle of 45° and is observed at a right angle to this direction, a distorted profile height h' (see fig. 3(b)) is observed instead of the real profile height h. Obviously,

$$\frac{h}{h'} = \sin 45^\circ = \sqrt{2} \qquad (1)$$

The factor $\sqrt{2}$ is accounted for in the course of movement of the reticle, making possible direct reading of measured values in the direction of the real profile height as well as in the longitudinal direction of the profile. The instrument has a range capability for measurement of surface irregularities from 1 to 400 microns in magnitude.

REFLECTANCE AND TEMPERATURE MEASUREMENT

Reflectance Measurement

The principles of operation and measurement employed by the image pyrometer are given in reference 4. In the following discussion they are summarized and the calculations involved are modified for application to measurements over a range of wavelengths. To determine the temperature of the sample it is first necessary to determine its emittance. For an opaque sample

$$\alpha_\lambda + \rho_\lambda = 1 \tag{2}$$

where α_λ and ρ_λ are the spectral absorptance and reflectance, respectively, and from Kirchoff's law (see ref. 6) and equation (2),

$$\epsilon_\lambda = \alpha_\lambda = 1 - \rho_\lambda \tag{3}$$

where ϵ_λ is the spectral emittance. The image pyrometer measures the spectral reflectance, from which the spectral emittance is calculated by equation (3) and used in the determination of sample temperature. To accomplish the reflectance measurement, the apparatus measures sequentially the arc light, the emitted plus reflected light from the sample, and the emitted light from the sample. (The difference between the last two measurements is the reflected light from the sample.) The emitted light from the sample is measured while arc irradiation of the sample is briefly obstructed by the chopper. Interruption by the chopper occurs every 65 milliseconds and the duration of each interruption is about 5 milliseconds.

From the foregoing considerations the spectral emittance may be expressed as

$$\epsilon_\lambda = 1 - \rho_\lambda = 1 - \frac{r_\lambda}{i_\lambda} = 1 - K\,\frac{(R_\lambda + E_\lambda) - E_\lambda}{A_\lambda} \tag{4}$$

where

r_λ = Reflected light from an element of sample surface

i_λ = Incident light on the same element of sample surface

K = A combined constant of the optical system

R_λ = Oscillographic indication of reflected light from the sample in arbitrary units

E_λ = Oscillographic indication of emitted light from the sample in arbitrary units

A_λ = Oscillographic indication of arc light in the same arbitrary units

The constant K includes a measure of the fraction of arc radiation in the midplane image that is incident on the sample. This constant may be determined by replacing the sample with a water-cooled surface of known reflectance. Because the spectral reflectance of freshly-deposited magnesium oxide has been extensively studied (see refs. 7 to 9), it was used in this measurement program as a standard. Its diffuse reflectance throughout the visible spectrum is about 0.97.

The reflectance measurement of the image pyrometer is essentially hemispherical spectral, including specular and diffuse components, since the angle of collection and re-imaging of the arc imaging furnace mirrors is 170° (minus a small angle about the axis of the mirrors). Hence, this apparatus makes a close approach to the measurement of reflectance as it is defined in its strictest sense. The emittance determined is essentially hemispherical spectral, since the complement of hemispherical emittance is reflectance under conditions of hemispherical illumination and hemispherical viewing.

Temperature Calculation

Calculation of the temperature of the sample requires comparative measurements between radiation from the sample and that from a standard temperature source. A tungsten-strip lamp serves as a standard source of constant and accurately-determined temperature. Planck's law or Wien's law may be written for the sample and for the standard lamp. Wien's law is simpler to use and was used here since the maximum error introduced, for the range of wavelengths and temperatures involved, was less than one-half of 1 percent (see ref. 10). Wien's law for the sample is

$$W_{\lambda s} = \frac{\epsilon_{\lambda s} c_1}{\lambda^5 e^{c_2/\lambda T_s}} \tag{5}$$

where $W_{\lambda s}$ is the hemispherical spectral radiant intensity per unit area of the sample, $\epsilon_{\lambda s}$ is the hemispherical spectral emittance of the sample at wavelength λ, and c_1 and c_2 are the first and second thermal radiation constants. $W_{\lambda s}$ is the time rate of emission of radiant energy per unit interval of wavelength throughout 2π steradians per unit of area of the sample at absolute temperature T_s.

Wien's law for the standard lamp is

$$W_{\lambda L} = \frac{\epsilon_{\lambda L} c_1}{\lambda^5 e^{c_2/\lambda T_L}} \tag{6}$$

where $W_{\lambda L}$ is the hemispherical spectral radiant intensity per unit area of the tungsten strip of the lamp, $\epsilon_{\lambda L}$ is the hemispherical spectral emittance of the lamp, and T_L is the true absolute temperature of the lamp. The left sides of the two Wien's law equations may be expressed in terms of the oscillographic measurements on sample and lamp. These measurements are related to the sample and lamp temperatures by the following expression:

$$\frac{1}{T_L} - \frac{1}{T_s} = \frac{\lambda}{c_2} \ln \frac{\epsilon_{\lambda L} E_{\lambda s}}{\epsilon_{\lambda s} E_{\lambda L}} \tag{7}$$

where $E_{\lambda L}$ is the standard lamp oscillographic amplitude in arbitrary units and the other symbols are as defined earlier. Solving equation (7) for T_s gives

$$T_s = \frac{T_L}{1 - k_\lambda T_L \log \frac{\epsilon_{\lambda L} E_{\lambda s}}{\epsilon_{\lambda s} E_{\lambda L}}} \tag{8}$$

where

$$k_\lambda = \frac{2.302\lambda}{c_2} = \text{A constant incorporating a change from natural to common logarithms and absorbing } \lambda/c_2 \tag{9}$$

The constant k_λ is a function of the filter and detector system in the pyrometer and is directly related to the effective wavelength of response of the image pyrometer. The value of k_λ may be determined by operation of the pyrometer with the standard lamp set successively at two different temperatures, T_{1L} and T_{2L}. The resultant expression for k_λ is

$$k_\lambda = \frac{T_{1L} - T_{2L}}{T_{1L} T_{2L} \log \frac{\epsilon_{2\lambda L} E_{1\lambda L}}{\epsilon_{1\lambda L} E_{2\lambda L}}} \tag{10}$$

where T_{1L} and T_{2L} are the higher and lower temperatures of the lamp, respectively, $\epsilon_{1\lambda L}$ and $\epsilon_{2\lambda L}$ are the spectral emittances of the lamp corresponding to the two temperatures, and $E_{1\lambda L}$ and $E_{2\lambda L}$ are the oscillographic amplitudes corresponding to the two temperatures. The value of k_λ thus determined can be used to determine the sample temperature by its substitution into equation (8) with the oscillographic data from the lamp at either temperature.

Because of the unavailability of spectral hemispherical emittance data on tungsten-strip lamps at high temperatures, spectral normal emittance data were used in equations (8) and (10). The spectral normal emissivity of tungsten ribbon filament has been the subject of considerable study because of its use as

a radiation standard. The data of DeVos (ref. 11) and Larrabee (ref. 12), covering a broad range of wavelengths and temperatures are considered the most reliable available. The data of DeVos were used here. Normal and hemsipherical emittance of tungsten are not equal because it does not emit in accordance with Lambert's cosine law, but studies by Worthing (ref. 13) and by Blau, et al (ref. 14) indicate that hemispherically-measured values would not be more than 6 or 7 percent greater than normally-measured values.

MEASUREMENT PROGRAM AND RESULTS

Optical Filters

The image pyrometer was delivered with an RCA 1P22 photomultiplier and a Corning No. CS2-59 red glass filter, with an effective wavelength of about 0.7 micron. In order to cover the entire visible spectrum, five filters spaced at nearly equal intervals throughout the visible spectrum and covering a narrow region of the near ultraviolet were selected or constructed. Two of the filters were a Kodak Wratten No. 18A glass filter and the Corning No. CS2-59 which was supplied with the image pyrometer. The other three filters were constructed by mounting Kodak Wratten gelatin film in Canada balsam cement between two thin layers of optically flat glass. These were Kodak Wratten Numbers 45 and 47B overlapped, Kodak Wratten Numbers 21 and 64 overlapped, and Kodak Wratten No. 70. Tests were made to assure that the temperature in the filter receptacle of the pyrometer during furnace operation stayed within safe limits for use of the Wratten filters. An RCA 1P21 photomultiplier was used with all the filters except the Kodak No. 70, which was matched with the RCA 1P22 photomultiplier.

The effective wavelength of measurement for each filter was determined by taking the triple product of the filter transmission curve, the photomultiplier relative response curve, and the relative spectral hemispherical radiant intensity curve for the standard lamp at 2,900° K to obtain a product curve representing the combined spectral response of the source-filter-detector system. As an example, figure 4 shows this determination for Kodak filter 18A. The area under the product curve was divided into two equal parts, and the dividing line was taken as the definition of the effective wavelength. The wavelength values determined by the above method were approximately 1 to 4 percent lower than those calculated by equation (9). Data were plotted as a function of the effective wavelength values determined from the product curves.

Temperature Control

The measurements of reflectance and temperature in this investigation were obtained in every case in the region of highest surface temperature on the sample, after the sample had attained steady-state conditions. In order to cover a range of temperatures, neutral-density filters were constructed of 10- and 20-mesh brass cloth to reduce the intensity of irradiation of the sample. Each wire cloth was mounted on a ring designed to fit the circumference of the mirror at the arc end of the arc imaging furnace, with a 6-inch-diameter hole in the region of the

arc. The purpose of this particular method of attenuation of the arc irradiation was to preserve the hemispherical character of the measurements and to avoid shadowing the midpoint image of the arc. It was believed this approach to temperature control would yield more reliable and consistent data than those obtainable from measurements during temperature rise or fall of the sample, or from measurements made at points across the temperature gradient that exists on the surface of the sample. Data covering a range of temperatures could be obtained by any of these methods with the image pyrometer.

Material Samples

Samples of all the materials studied were discs 1/2 inch in diameter and 3/16 inch in thickness. For each temperature and reflectance measurement, one of the discs was mounted in a small steel block, the sample being supported in and insulated from the block by four equally spaced, spring-loaded zirconia pins of 7/64-inch diameter, sharpened at the points of contact with the periphery of the sample. Measurements were made on one circular face of the disc, which was located in the minor focal plane of the re-imaging mirror with its center on the optical axis of the arc imaging furnace mirrors.

Surface-Roughness Measurement

Measuring surface roughness and expressing the measurements quantitatively in terms that are directly relatable to emittance or reflectance is a difficult problem. Standard surface-roughness parameters, such as arithmetical or root-mean-square average deviation from the center line or roughness width (for definitions, see ref. 15), inadequately define a surface for light-reflecting or light-emitting purposes, because several surfaces may have identical values of these parameters and yet have different reflecting or emitting characteristics. A rather general practice in the field of emittance measurement is to define the surface properties of a material by describing the method of surface preparation previous to the emittance measurement. Perhaps this approach has merit but its limitations are apparent, since it is the microgeometry of the surface itself rather than the method of surface preparation that is potentially relatable to emittance and reflectance. For ambient- or low-temperature measurements the surface finish may retain its initial character throughout the history of the emittance-measurement operation, but for measurements at high temperatures the surfaces of many materials will experience alterations which will in most cases depend on the particular environment surrounding the sample. It appears that emittance data can be more meaningfully defined by describing previous surface treatment and, in addition, describing the surface finish following the measurement. The experimental difficulty and perhaps impracticality of obtaining simultaneous emittance and surface-roughness data on a sample at elevated temperature is recognized. However, in many cases, changes occurring in surface conditions are most pronounced during the heating or soaking part of the temperature cycle, and measurements of surface roughness at termination of the emittance measurement and cooling of the sample represent the surface at elevated temperature, except for thermal expansion. An attempt has been made in the present investigation to define surface preparation on samples before testing and to define the surface roughness following the reflectance measurements. Measurements of surface

roughness were obtained with a Carl Zeiss Light-Section Microscope, the operation principles of which were discussed earlier, and the measurements were treated by a statistical method suggested by Posey (ref. 16) which seems to characterize the roughness of a profile quite completely. Three curves are employed (e.g., see fig. 9). One is an x-y profile curve formed from the microscope measurements, the ordinates y representing the varying distances of the profile above a base line passing through the deepest valley of the profile, and the abscissas x representing distances along the profile measured parallel to the base line. A second curve, representing the slope of the profile, is a plot of values of $y' = dy/dx$, and a third curve is a plot of values of $y'' = d^2y/dx^2$, which represents approximately the degree of curvature of the x-y profile for small values of y'. By dividing the range of values of y into several equal increments and determining the percentage of the total distance x for which the curve lies within each increment, a histogram of y-values can be plotted in the y-direction at the right end of the x-axis. Similarly, histograms can be formed to represent the slope distribution and degree-of-curvature distribution.

Measurements on Carbon and Graphite

Spectral emittance and reflectance data were obtained on National Carbon Company's AGKSP graphite and L113SP carbon, both high-purity spectroscopic grades of materials, at three temperature levels. To assure that all samples of each material had like surfaces before testing, the surface of each graphite and carbon disc to be exposed to the furnace radiation was polished successively with 0, 3/0, and 4/0 grades of emery polishing paper, resulting in a final glossy finish. Upon exposure in air to the arc image thermal flux, this surface quickly oxidized to a stably rough surface. Each sample was exposed for approximately the same length of time at each temperature level. In every case the exposure was long enough for the sample to attain its maximum steady-state temperature but not long enough to permit appreciable recession of the surface on which the image pyrometer measurements were being made. Varying arc irradiation level from conditions of no attenuation to that produced by the 20-mesh filter, average temperatures varied from 5,275° F to 3,285° F on carbon and from 4,855° F to 3,250° F on graphite, as shown in figures 5 to 8, where emittance and reflectance data are presented as a function of wavelength for each temperature and as a function of temperature for each wavelength. Duplicate measurements were made for each particular set of conditions, with the exception that triplicate measurements were made on graphite at its highest temperature.

The spectral emittance measured at the 5,000° F temperature level is nearly constant for both graphite and carbon from 0.37 micron to about 0.55 micron, being about 0.96 for graphite and 0.97 for carbon, and beyond this wavelength it decreases gradually to about 0.89 for both materials. At lower temperatures the materials also show a decrease in emittance with increasing wavelength in the red part of the spectrum and a tendency toward increasing emittance with decreasing temperature. Directional measurement of spectral reflectance at a 45° angle from the normal to the material surface on these same grades of graphite and carbon under similar test conditions by Null and Lozier (ref. 17) produced values of emittance in reasonable agreement with those obtained in this investigation, for the spectral range common to the two sets of data. Although Null and Lozier did

not report data beyond about 0.60 micron, they indicated that their measurements had shown a trend toward increasing reflectance at longer wavelengths, and the measurements of other investigators also have shown this trend, as indicated in reference 18.

Surface-roughness data on graphite and carbon are presented in figures 9 and 10, where y, y', and y" are plotted as a function of x at x-intervals of 25 microns and their histograms are shown at the right ends of the curves. The roughness measurements covered a 1,225-micron length of surface near the center of the surface on which the emittance measurements were made. This length is about 1/10 the diameter of the sample.

Measurements on Zirconia

Zirconia emittance samples were machined from Norton Company's RZ-5723 zirconia (94.57 percent ZrO_2, 3.73 percent CaO), supplied in 1/2-inch-diameter rod. The rod was cut into discs, the surfaces of which were finished with a N100-0220 diamond wheel. After the machining operation the samples were ultrasonically cleaned in distilled water. Attenuation of the arc irradiation with the 10-mesh filter was sufficient to just melt a small spot of about 1/8-inch diameter on the center of the sample surface. Under these conditions the temperature measured would be expected to be very close to the melting point of zirconia. The temperature values measured at four different wavelengths ranging from 0.46 micron to 0.72 micron averaged 4,895° F with only about a 1-percent maximum deviation from this for the eight tests shown in the lower curve of figure 11. Reported values for the melting temperature of zirconia (see refs. 19, 20, and 21) range from 4,850° F to 4,920° F. The consistency of the data obtained here with those reported in the literature attests to the temperature-measurement reliability of the image pyrometer. Few spectral emittance data are available on zirconia at temperatures between 4,000° F and 5,000° F. Cox (see ref. 22) has reported unidirectional measurements at 0.665 micron. His data at 4,350° F are about 7 or 8 percent lower than those found in this investigation.

Emittance and temperature were determined for diamond-wheel-finished samples of zirconia using the 20-mesh filter, and the results are shown as a function of wavelength in the upper curve of figure 11.

Special roughness treatments were given to samples of the diamond-wheel-finished zirconia to provide three gradated rougher surfaces. The roughest was obtained by grit blasting with Norton No. 90-120 ZrO_2 grit and the other two surfaces with No. 120-150 and No. 150F grit. Emittance and temperature were determined with the 20-mesh filter to maintain the temperature below the melting point, and at wavelengths of 0.46 micron and 0.65 micron. Emittance measurements on the three grit-blasted surfaces were essentially the same for each wavelength and did not differ significantly from those values measured on the diamond-wheel-finished surfaces, as can be seen in figure 11. The four gradations of surface roughness are demonstrated in figures 12 to 15. There appear to be no large differences among the four profile-slope distributions and the four profile-curvature distributions. There are noticeable differences among the y-distributions, and the maximum peak-to-valley depth of the diamond-wheel-finished surface is only

about half the values for the three grit-blasted surfaces. No attempt is made herein to assess the significance of differences or similarities among the distributions of any one type with respect to emittance. The independence of measured reflectance and calculated emittance on the roughness differences exhibited here indicates that there is no significant influence of such roughness differences on the emittance of zirconia in the visible spectrum.

The explanation for the independence of emittance on surface roughness may lie in the transmission characteristics of zirconia for limited thicknesses of the material. The transmittance of zirconia for visible radiation at high temperatures is not well known, but it is indicated in reference 22 that the thickness required for opacity varies from about 0.16 inch at room temperature to 0.05 inch at the melting point. It can be seen from the surface profile data in figures 12 to 15 that the maximum values of y are much less than 0.05 inch (1,250 microns), and consequently, the irregularities in the surface would have little influence on the emittance and reflectance if zirconia has high transmittance up to this thickness. Another possible factor in the behavior is that for some types of surfaces, emittance and reflectance may be little influenced by the surface roughness when these quantities are measured hemispherically for hemispherical illumination. Unidirectional measurements at some particular angle might show influences of surface roughness that would be averaged out in hemispherical measurements. Further experimental and/or analytical studies would be required to verify or nullify this possibility.

Surface-roughness data are not presented on the melted zirconia surface because the maximum values of y were of the order of one micron, the lower limit of measurement of the light-section microscope.

Measurements on Phenolic-Nylon Ablation Char

A phenolic-nylon was chosen as the ablation material for study in this program. The phenolic-nylon was molded from a mixture of 50 percent by weight of phenolic resin and 50 percent by weight of nylon powder. The density in molded form was about 75 lb/ft^3. The phenolic-nylon was thermally reacted by two different methods to form char residue. In one case the material was heated in an oven which was constantly purged with nitrogen at a pressure slightly greater than atmospheric. The oven was controlled to produce an average rate of temperature rise of 75° F/hr until the material reached $1,500^\circ$ F. The material was sustained at this temperature for three hours and then cooled to room temperature at a rate equal to the temperature-rise rate. The density of the char formed was about 38 lb/ft^3. The phenolic-nylon was reacted in cylindrical form and the charred cylinders were subsequently cut by standard machining operations into discs for emittance samples. These discs were given no special surface treatments.

In the other case 3-inch-diameter discs of the phenolic-nylon were exposed to an electric-arc-heated subsonic stream of nitrogen for 165 seconds, the time required to produce a char layer of about 3/16-inch thickness. The arc jet, described more completely in reference 2, was operated with a 2-inch-diameter nozzle and with arc power of 1,000 kilowatts. Under these operating conditions the arc jet produced an aerodynamic thermal flux of about 100 Btu/ft^2-sec on the phenolic-nylon discs located 2 inches from the nozzle. The maximum surface temperature attained by the char layers during their formation was about $3,000^\circ$ F.

The density of the chars was 21 lb/ft^3. Discs of 1/2-inch diameter were cut from the char layers for emittance samples. The discs were given no special surface preparation, and reflectance measurements were made on the surface that had been exposed to the arc-heated nitrogen stream.

There is a considerable difference in the densities of the chars produced by the two different methods of heating. The two chars are different in appearance, the most distinctive feature being the columnar structure of the arc-jet-formed char, produced by the rapidly escaping gases as they flow from the zone of reaction through the growing char layer, as contrasted with the homogeneous structure of the oven-formed char. The chars produced in the arc jet undergo a reaction process which is more simulative of the actual conditions of ablation char formation on reentry vehicle heat shields than that of the oven-produced chars. It is difficult to obtain chars formed under dynamic heating conditions in any form other than relatively thin layers. On the other hand, chars can be formed in a greater variety of shapes and sizes under static heating conditions. Standard methods of measuring thermal conductivity, thermal expansion, specific heat, and other thermal properties require samples of geometry not readily obtainable from material in thin-sheet form. The desirability for measurement of such properties of chars to acquire a more complete understanding of ablation-type thermal protection systems produces an interest in the similarity or dissimilarity of thermal-physical properties of chars produced by different methods. The two differently-formed chars were investigated here to determine whether the emittance is significantly influenced by the method of char formation. A nitrogen environment was used in both reaction methods to prevent loss of chars from oxidation.

The emittance and reflectance of the chars are shown as a function of wavelength and temperature in figures 16 to 19. In general, the emittance of the oven-produced char is slightly higher than the arc-jet-produced char. Both bear a resemblance to graphite and carbon, in that the emittance drops in the red region of the spectrum and in that there is a tendency toward decreasing emittance with increasing temperature. The resemblance of emittance-temperature patterns of the chars to those of graphite and carbon is not unexpected, inasmuch as the chars themselves are carbonaceous.

Under identical test conditions higher surface temperatures were measured on the chars than those measured on graphite and carbon. All the measurements were made in air at atmospheric pressure, and a plausible explanation for the higher char temperatures is that the porosity of the chars rendered them more susceptible than carbon and graphite to rapid oxidation. The rapid exothermic oxidation process would increase the sample temperature beyond that expected for conditions of less severe or no oxidation.

Surface-roughness data on the chars are presented in figures 20 and 21. The roughness measurements were made on samples for which emittance measurements had been made at the highest temperatures.

EVALUATION OF RESULTS

No attempt was made in this investigation to determine the absolute accuracy of the measurements obtained because of the lack of high-temperature reference standards. All the results presented are considered reliable. Reasonable agreement has been shown to exist between the results reported here and data reported by other recent investigators. In general, measurements on like samples of a material were closely reproducible.

Certain additional unreported measurements of surface roughness on carbon were made to determine whether a 1,225-micron length of profile was sufficient to accurately represent the surface and to determine whether the carbon sample measured was typical. The histogram results were not appreciably changed when the length of profile examined was doubled, and histograms of two separate samples which had experienced like test conditions showed no significant difference. It is assumed that similar additional measurements on the other materials studied would also be consistent with those that were measured and reported. Since the geometries of the surfaces studied here are expected to be randomly irregular, with no directional surface qualities, the limitation of the roughness measurements to one arbitrary direction is considered sufficient. Arc-image heating of the sample was instantaneously terminated at the end of each reflectance measurement, and subsequently surface-roughness measurements were made. Therefore, the roughness measurements should be a good representation of surface conditions during reflectance measurement.

Surface-roughness data are included in this study primarily as a suggested method of more completely defining emittance data, with no attempt here to directly relate emittance and surface roughness. However, it is believed that data of the type presented here are sufficient to determine the dependence of emittance (hemispherical or unidirectional) on surface roughness for any particular material, if the emittance of a specularly-reflecting surface element of the material and the geometrical distribution of emitted radiation for all directions over a hemisphere are known for the element of surface.

For values of the slope greatly different from zero, y'' does not closely approximate the curvature of the x-y profile. Analytical use of the surface-roughness data probably would require determination of the true curvature from the corresponding y'- and y''-values.

It is not possible, at the present time, to predict the total radiation characteristics of the phenolic-nylon ablation material chars because only about 20 percent of the total radiation from a black body at $6,000^{\circ}$ F lies within the visible spectrum. The data obtained in this study would have to be supplemented with additional data extending to about 3 microns to give a picture of total emittance characteristics. Such data could conceivably be obtained from the image pyrometer with certain innovations.

Spectral emittance is equivalent to spectral absorptance at a particular temperature. Therefore, the data reported herein are potentially useful for evaluation of the absorptance of phenolic-nylon char for radiation from any source

emitting strongly in the visible spectrum. In particular, a significant part of the energy spectrum of radiation from shock-heated air associated with certain types of reentry operations may be in the visible region.

CONCLUDING REMARKS

Special optical techniques have been applied to emittance studies on materials at high temperatures and have been shown to be useful for obtaining emittance and temperature data on ablation material chars needed for assessing their performance in thermal protection systems of space vehicles. The investigation consisted of an evaluation of a recently-developed method of measuring reflectance and temperature, with adaptation and use of the method for obtaining measurements of spectral reflectance on certain carbonaceous and ceramic materials over a wavelength range from 0.37 to 0.72 micron and over a temperature range from 3,000° F to 6,000° F. The microgeometries of the surfaces on which reflectance was measured were statistically defined.

The apparatus employed for reflectance and temperature measurement was an Arthur D. Little-Strong Arc Imaging Furnace and an image pyrometer designed for operation in conjunction with the ellipsoidal arc imaging furnace. As a part of the evaluation of the experimental apparatus, measurements of the reflectance of graphite and carbon were made for the comparison of results with the data of other recent investigators of these materials. The results obtained agreed reasonably with those of the other investigators. In addition, measurements were made on zirconia at its melting point to confirm the temperature-measurement accuracy of the image pyrometer, within the accuracy with which the melting point of zirconia has been determined.

Hemispherical spectral emittance (absorptance) of phenolic-nylon ablation char was determined at wavelengths from 0.37 to 0.72 micron and at temperatures from 4,000° F to 6,000° F. If these data are supplemented with additional infrared data, the thermal radiation properties of the char for the associated temperature range can be completely determined and used in assessing its efficiency in radiation cooling. Relatedly, the data obtained here can be used to determine the absorptance of the char for visible radiation from shock-heated air associated with certain types of reentry operations.

An attempt was made to qualify the emittance data on all the materials with surface-roughness data pertinent to the time at which emittance was determined. Measurements of surface roughness were performed with a Carl Zeiss Light-Section Microscope, and the measurements were statistically treated to yield data that appear amenable to analytical study relating emittance and surface roughness.

14. Blau, Henry H., Jr., Chaffee, Eleanor, Jasperse, John R., and Martin, William S.: High Temperature Thermal Radiation Properties of Solid Materials. Scientific Report Number 2, Contract AF19(604)-2639, March 31, 1960.

15. Surface Texture: Surface Roughness, Waviness, and Lay. ASA B46.1-1962, American Society of Mechanical Engineers, 1962.

16. Posey, C. J.: Measurement of Surface Roughness. Mechanical Engineering, Vol. 68, April 1946, pp. 305-306, 338.

17. Null, M. R., and Lozier, W. W.: Measurement of Spectral Reflectance and Emissivity of Specular and Diffuse Surfaces in the Carbon Arc Image Furnace. Research Laboratory, National Carbon Company, A Conference on Imaging Techniques, Arthur D. Little, Inc., Cambridge, Mass., Oct. 4-5, 1962.

18. Thorn, R. J., and Winslow, G. H.: Radiation of Thermal Energy from Real Bodies. Temperature - Its Measurement and Control in Science and Industry, Vol. 3, Part 1, Reinhold Publishing Corporation, New York, 1962, pp. 429-433.

19. Handbook of Chemistry and Physics. Forty-Second Edition, The Chemical Rubber Publishing Co., 1960-1961.

20. Thermal Properties of Solids. Vought Astronautics, CVA Report AST-E9R-12073, September 1959.

21. Handbook of Thermophysical Properties of Solid Materials. Vol. 3, Edited by Alexander Goldsmith, Thomas E. Waterman, and Harry J. Hirschhorn, The Macmillan Co., New York, 1961.

22. Cox, R. L.: A Technique for Measuring Thermal Radiation Properties of Translucent Materials at High Temperature. Vought Astronautics Division, Chance Vought Corporation, Symposium on Measurement of Thermal Radiation Properties of Solids, Dayton, Ohio, Sept. 5-7, 1962.

REFERENCES

1. Brooks, William A., Jr., Wadlin, Kenneth L., Swann, Robert T., and Peters, Roger W.: An Evaluation of Thermal Protection for Apollo. NASA TM X-613, 1961.

2. Peters, Roger W., and Wilson, R. Gale: Experimental Investigation of the Effect of Convective and Radiative Heat Loads on the Performance of Subliming and Charring Ablators. NASA TN D-1355, 1962.

3. Glaser, Peter E.: Imaging-Furnace Developments for High-Temperature Research. Journal of the Electrochemical Society, Vol. 107, 1960, pp. 226-231.

4. Comstock, Daniel F., Jr.: Method for Temperature and Reflectance Determination in an Arc Imaging Furnace. Temperature - Its Measurement and Control in Science and Industry, Vol. 3, Part 2, Reinhold Publishing Corporation, New York, 1962, pp. 1063-1071.

5. Abbott, E. J., and Goldschmidt, Edgar: Surface Quality: A Review of 'Technische Oberflächenkunde' by G. Schmaltz. Mechanical Engineering, Vol. 59, Nov. 1937, pp. 813-825.

6. Weinstein, M. A.: On the Validity of Kirchoff's Law for a Freely Radiating Body. American Journal of Physics, Vol. 28, 1960, pp. 123-125.

7. Standard Method of Preparation of a Magnesium Oxide Standard for Spectral Reflectivity. ASTM Designation D 986-50, ASTM Standards, 1961, Part 6, pp. 225-227.

8. Preparation and Calorimetric Properties of a Magnesium Oxide Reflectance Standard. National Bureau of Standards Letter Circular LC-547, March 1939.

9. Middleton, W. E. Knowles, and Sanders, C. L.: The Absolute Spectral Diffuse Reflectance of Magnesium Oxide. Journal of the Optical Society of America, Vol. 41, no. 6, June 1951.

10. Harrison, Thomas R.: Radiation Pyrometry and Its Underlying Principles of Radiant Heat Transfer. John Wiley & Sons, Inc., New York-London, 1960, p. 17.

11. DeVos, J. C.: A New Determination of the Emissivity of Tungsten Ribbon. Physica, Vol. 20, 1954, pp. 690-714.

12. Larrabee, Robert D.: Spectral Emissivity of Tungsten. Journal of the Optical Society of America, Vol. 49, June 1959, pp. 619-625.

13. Worthing, A. G.: Temperature, Its Measurement and Control in Science and Industry. Reinhold Publishing Corporation, New York, 1941, pp. 1164-1167.

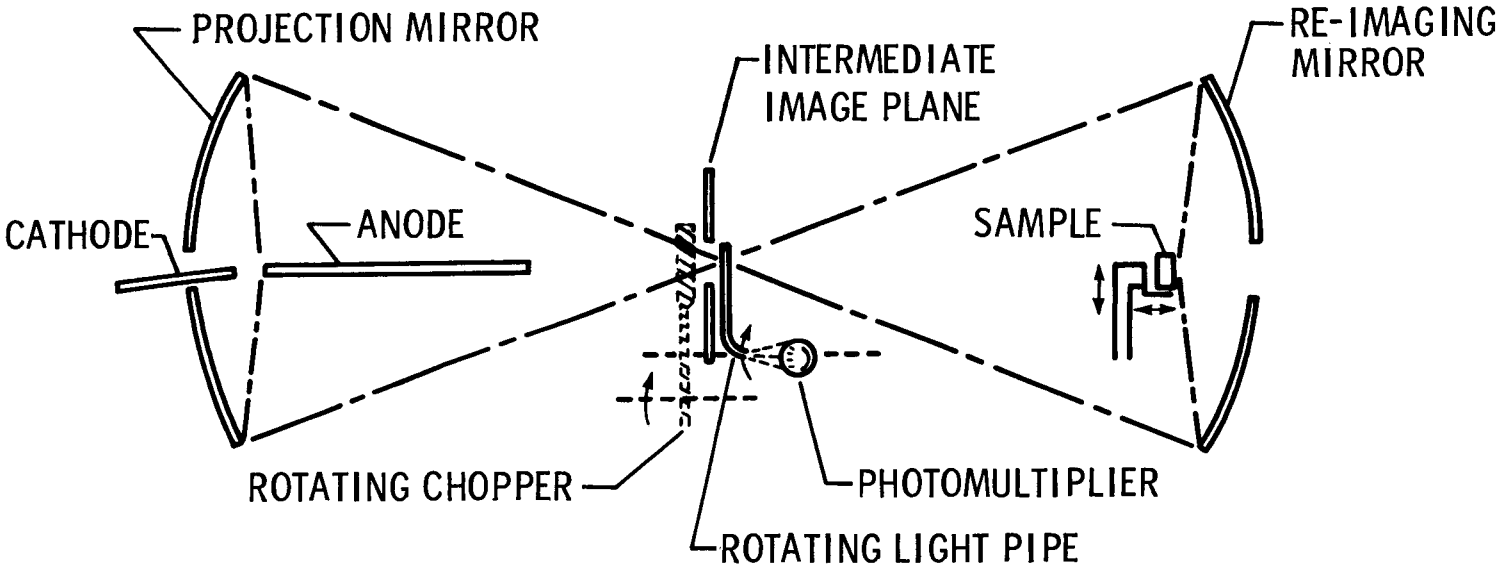

NASA

Figure 1.- Schematic of Arthur D. Little-Strong arc imaging furnace with image pyrometer.

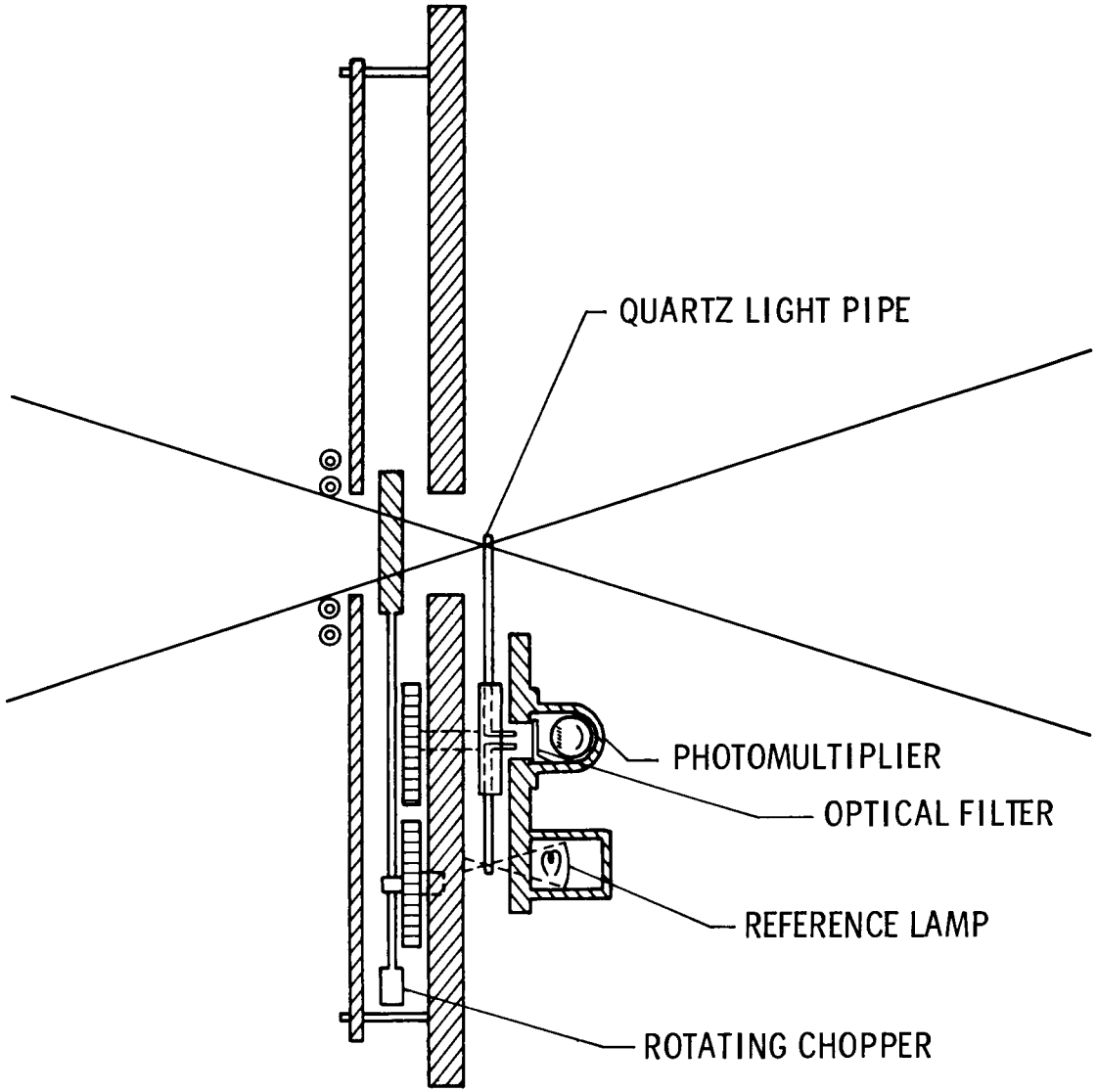

NASA

Figure 2.- Arthur D. Little image pyrometer operating mechanism.

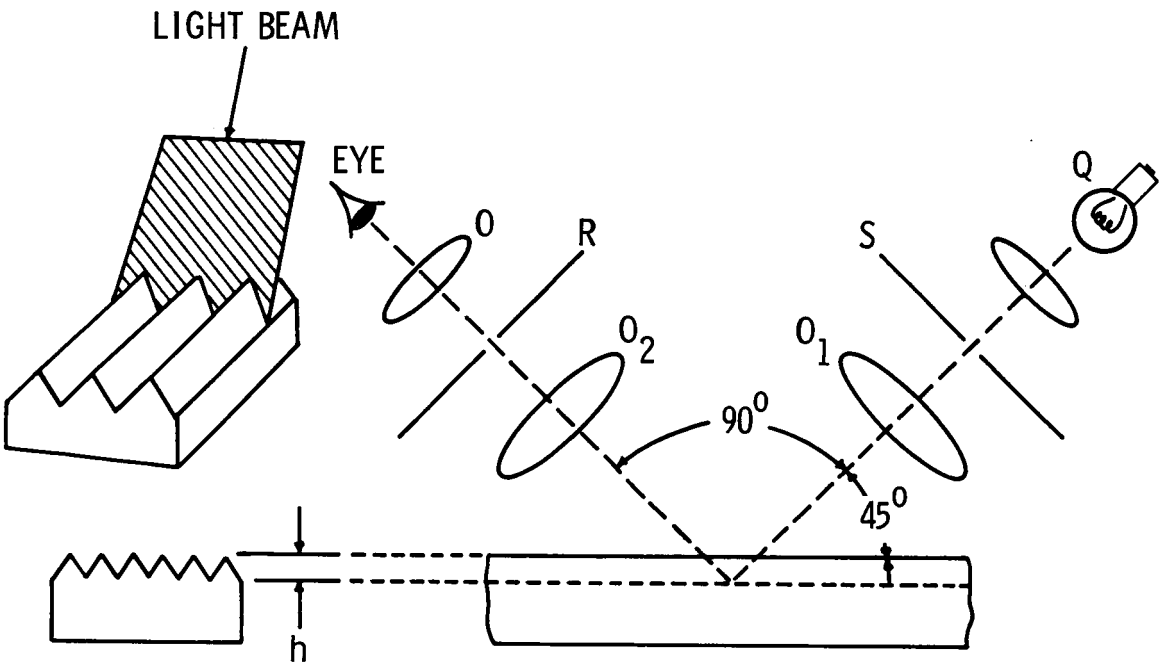

(a) Optical arrangement.

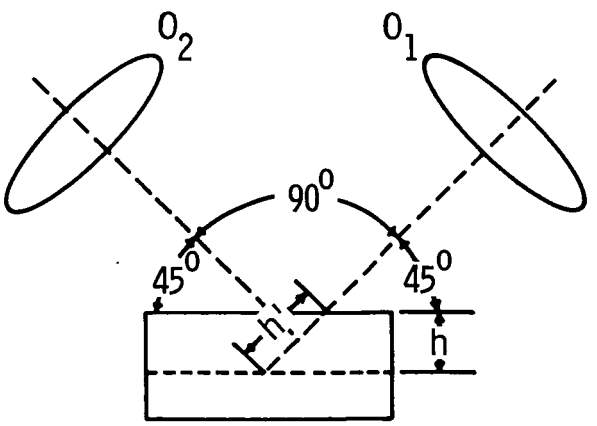

(b) Principle of measurement.

NASA

Figure 3.- Operation principles of light-section microscope.

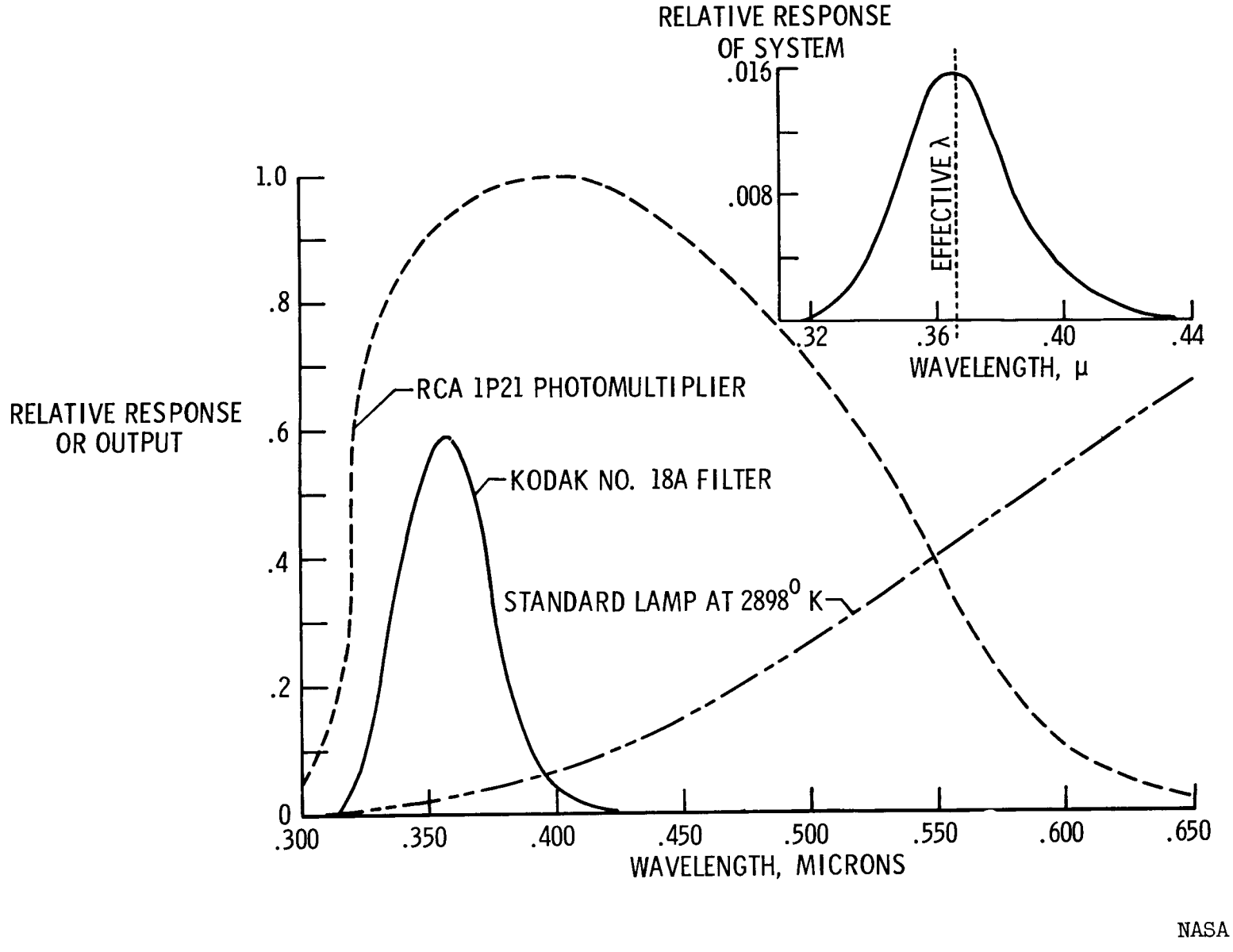

Figure 4.- Response of source-filter-detector system versus wavelength.

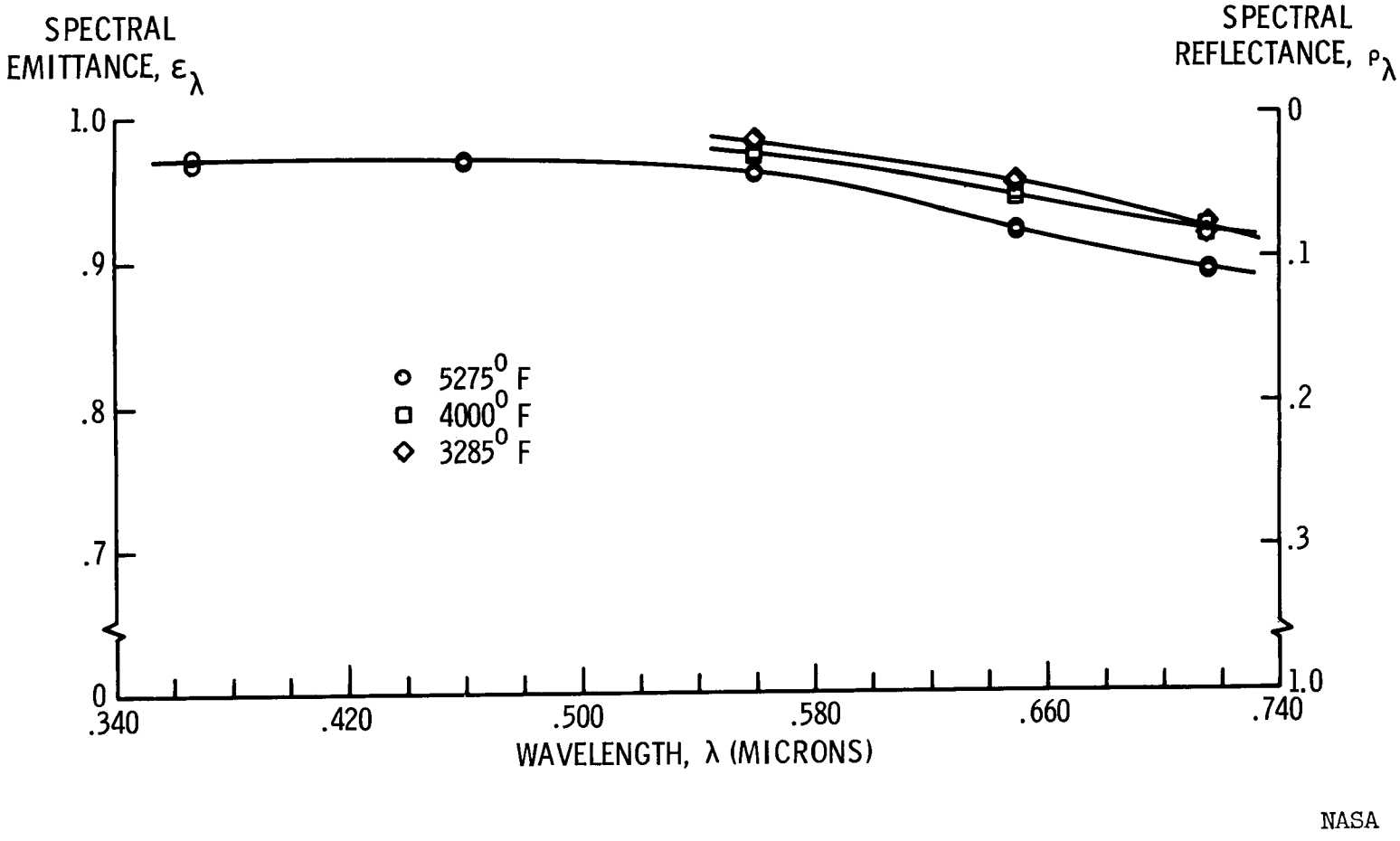

Figure 5.- Spectral emittance and reflectance of oxidized L113SP carbon versus wavelength.

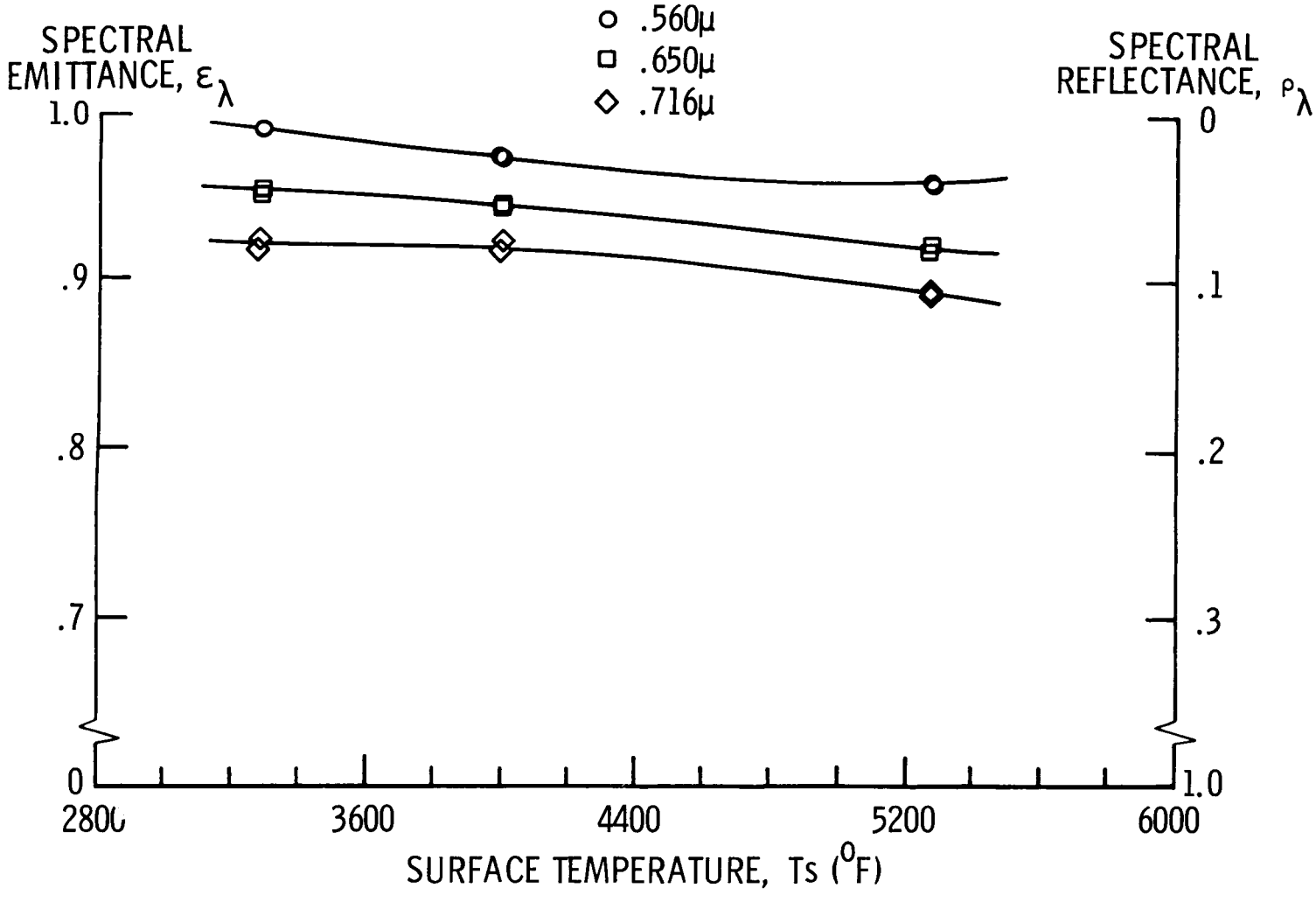

Figure 6.- Spectral emittance and reflectance of oxidized L113SP carbon versus temperature.

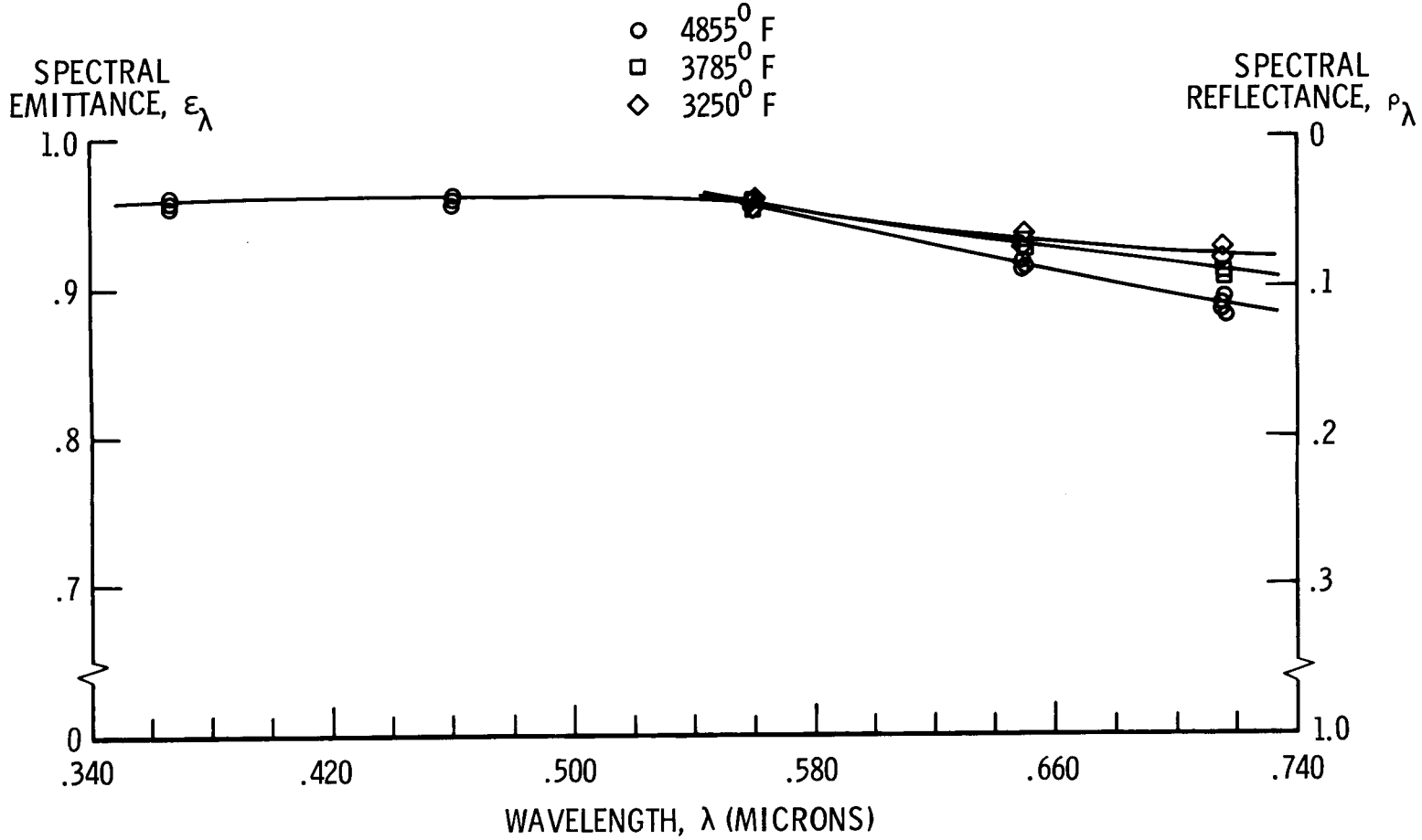

Figure 7.- Spectral emittance and reflectance of oxidized AGKSP graphite versus wavelength.

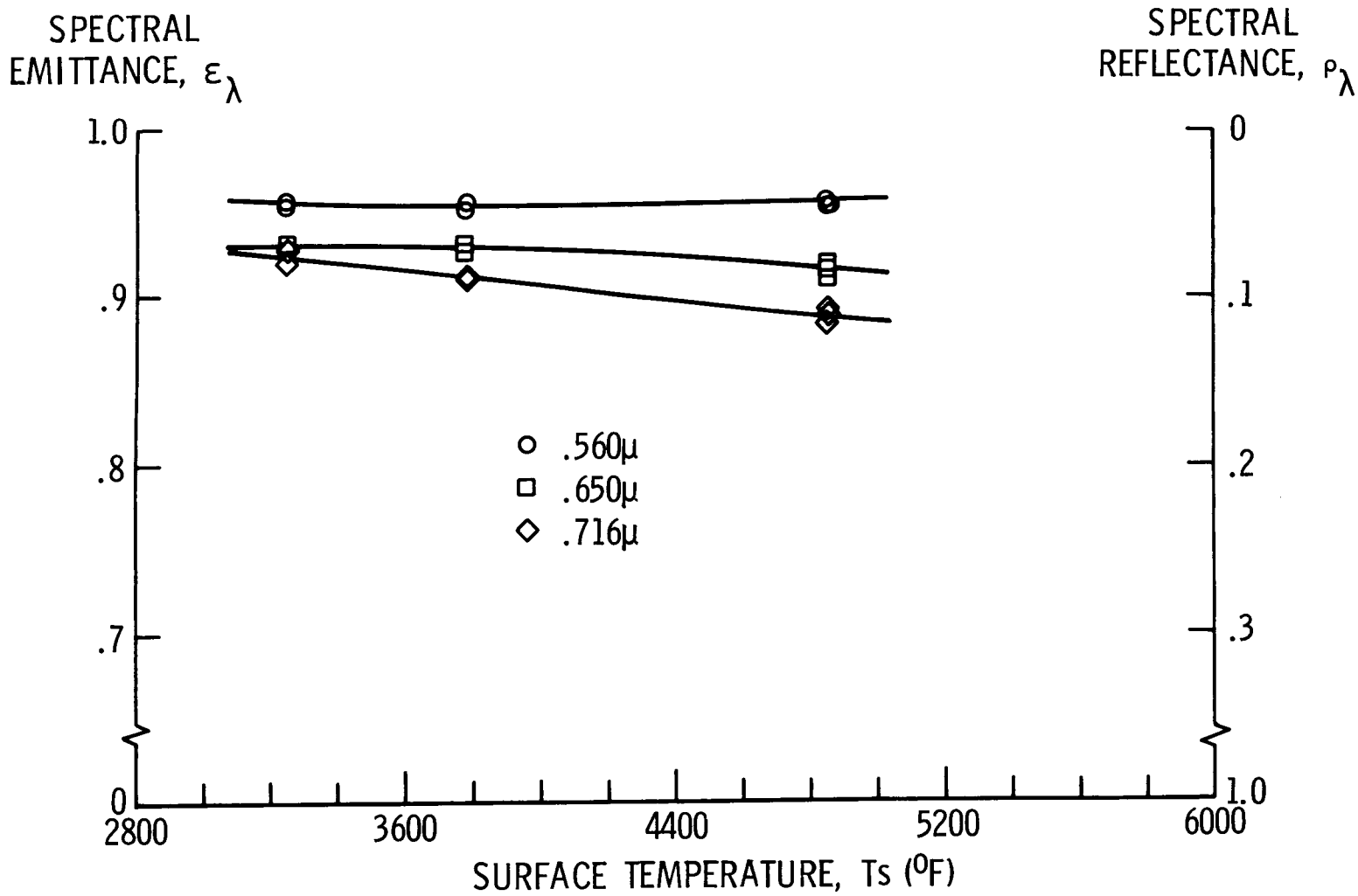

Figure 8.- Spectral emittance and reflectance of oxidized AGKSP graphite versus temperature.

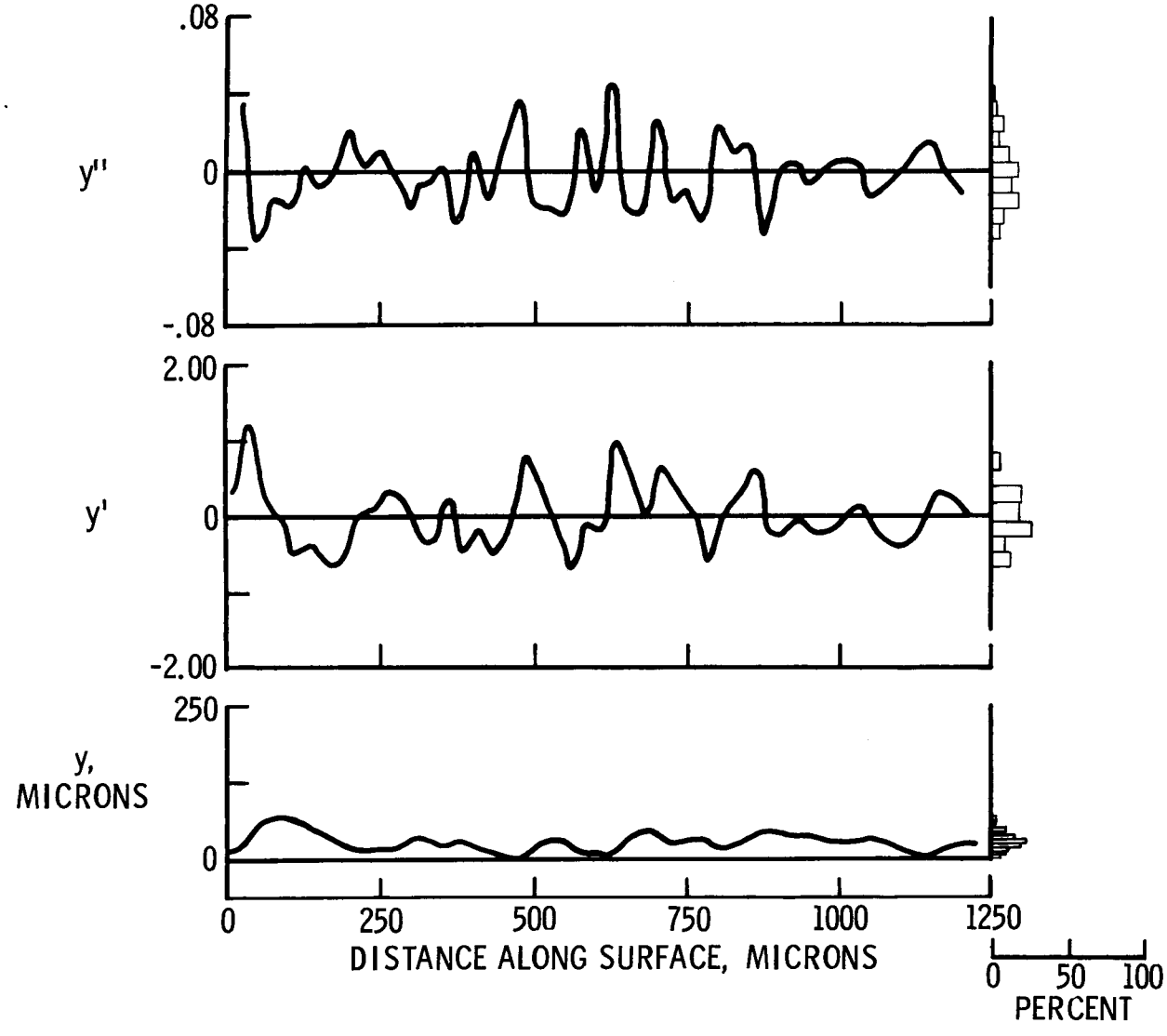

NASA

Figure 9.- Surface roughness of oxidized L113SP carbon.

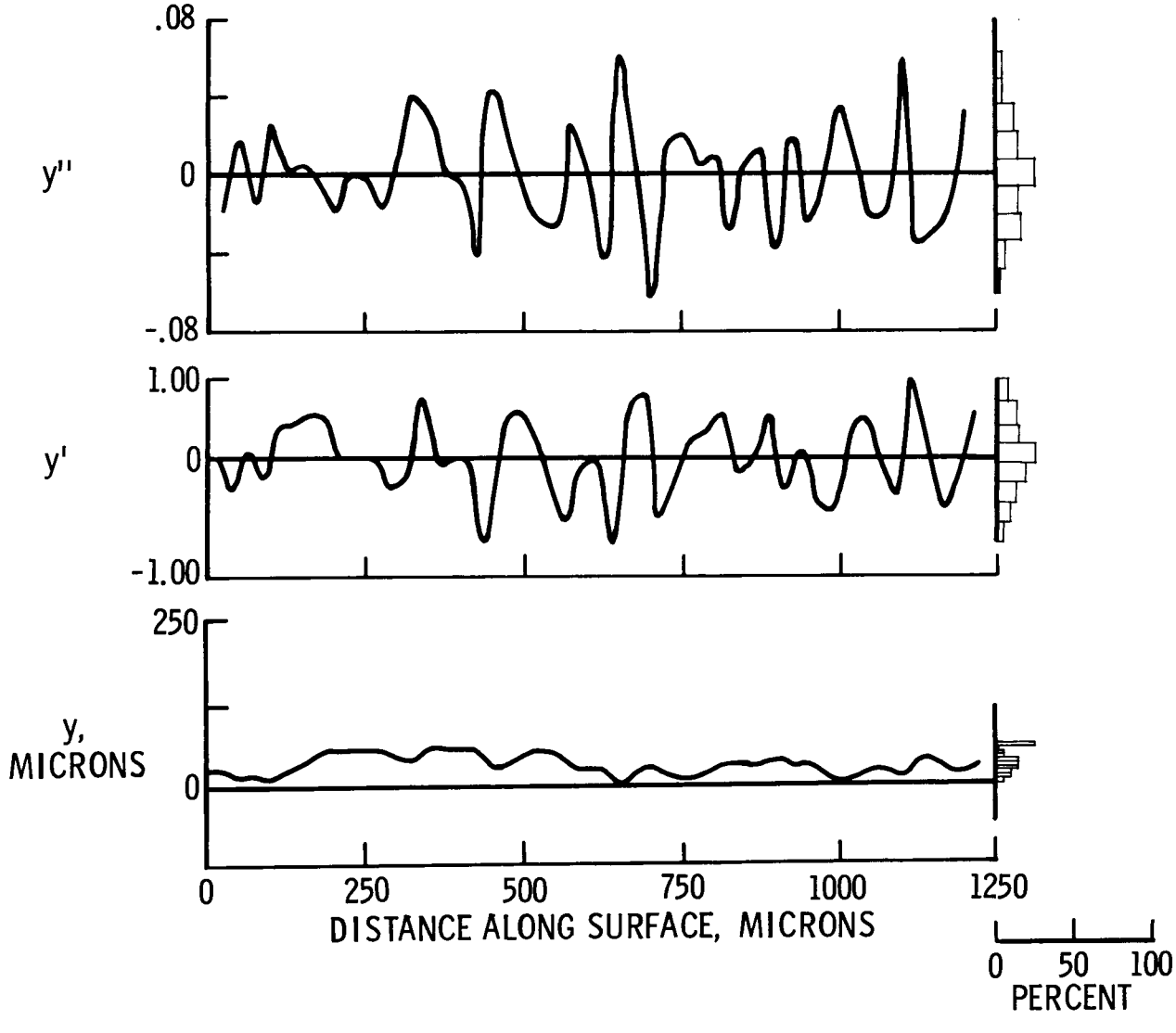

NASA

Figure 10.- Surface roughness of oxidized AGKSP graphite.

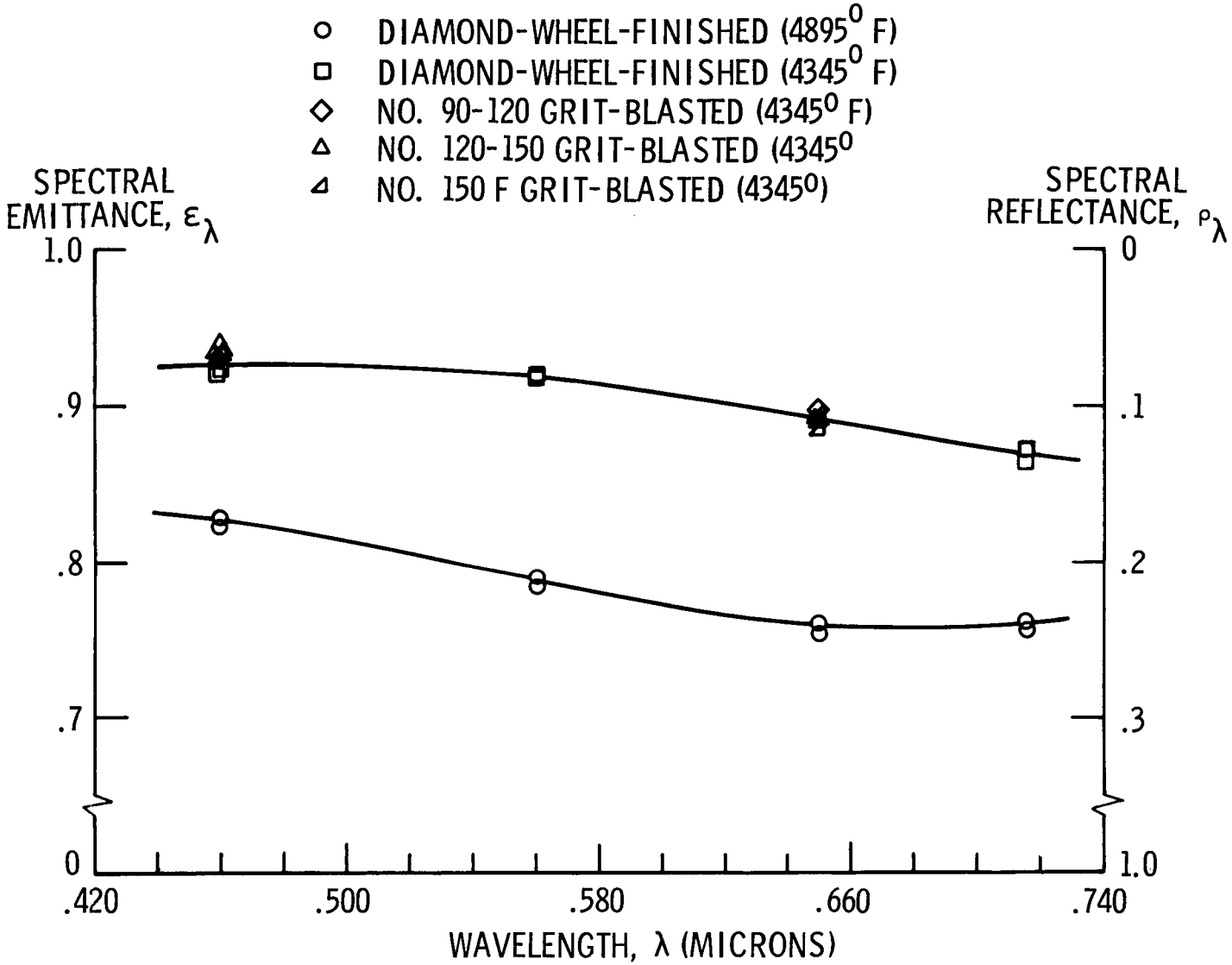

NASA

Figure 11.- Spectral emittance and reflectance of zirconia versus wavelength.

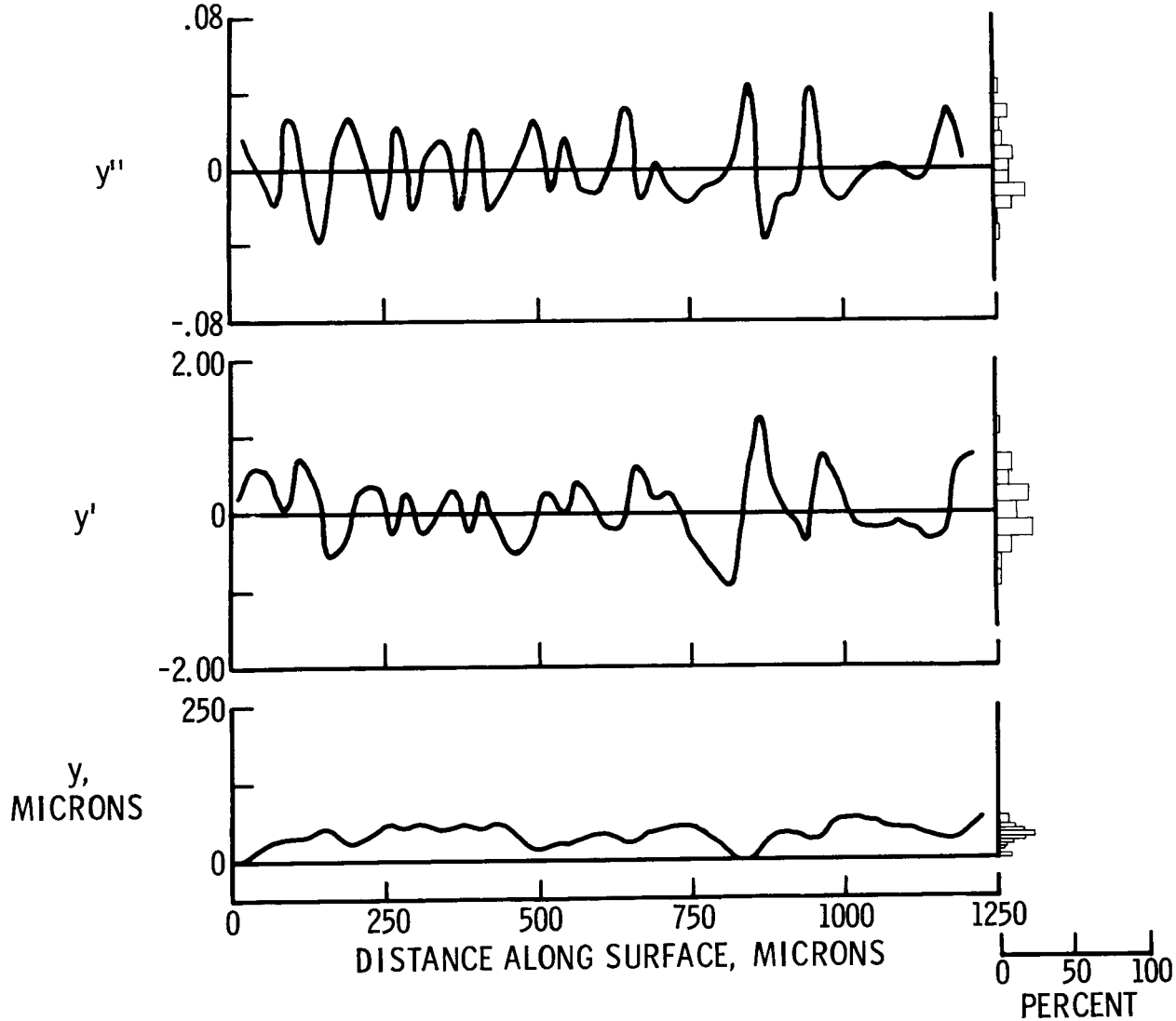

NASA

Figure 12.- Surface roughness of zirconia finished with diamond wheel.

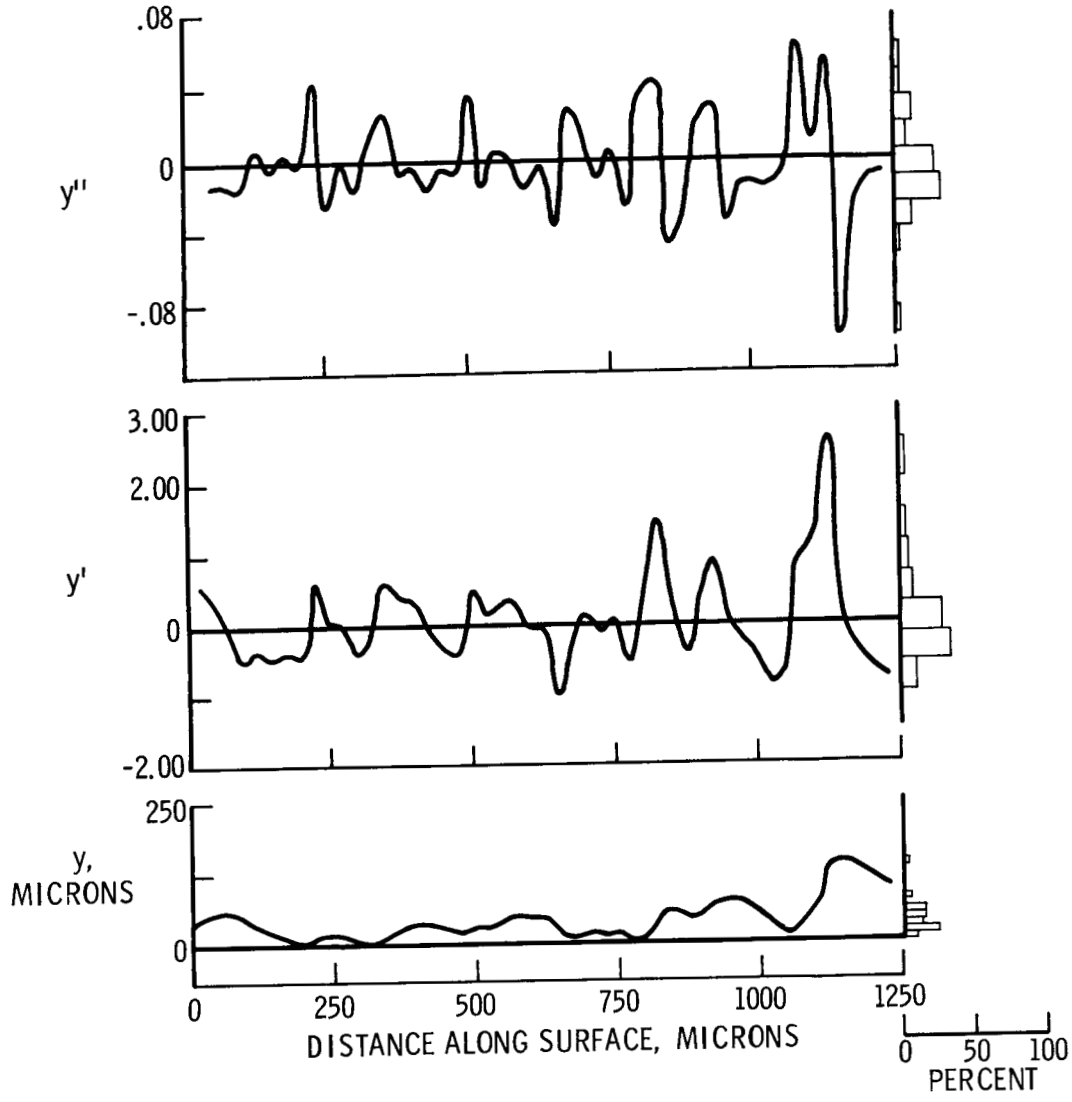

NASA

Figure 13.- Surface roughness of zirconia grit-blasted with No. 90-120 grit.

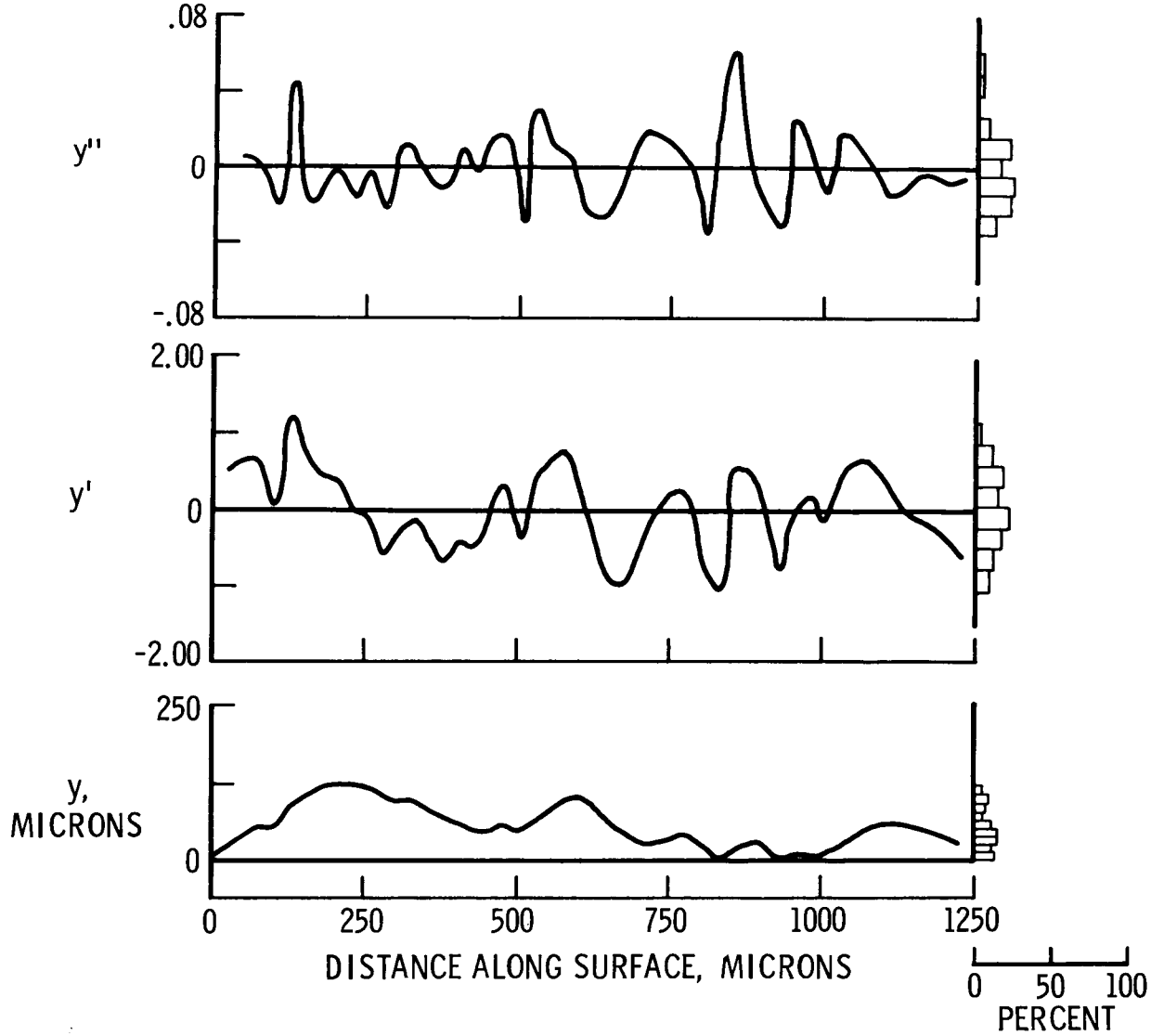

NASA

Figure 14.- Surface roughness of zirconia grit-blasted with No. 120-150 grit.

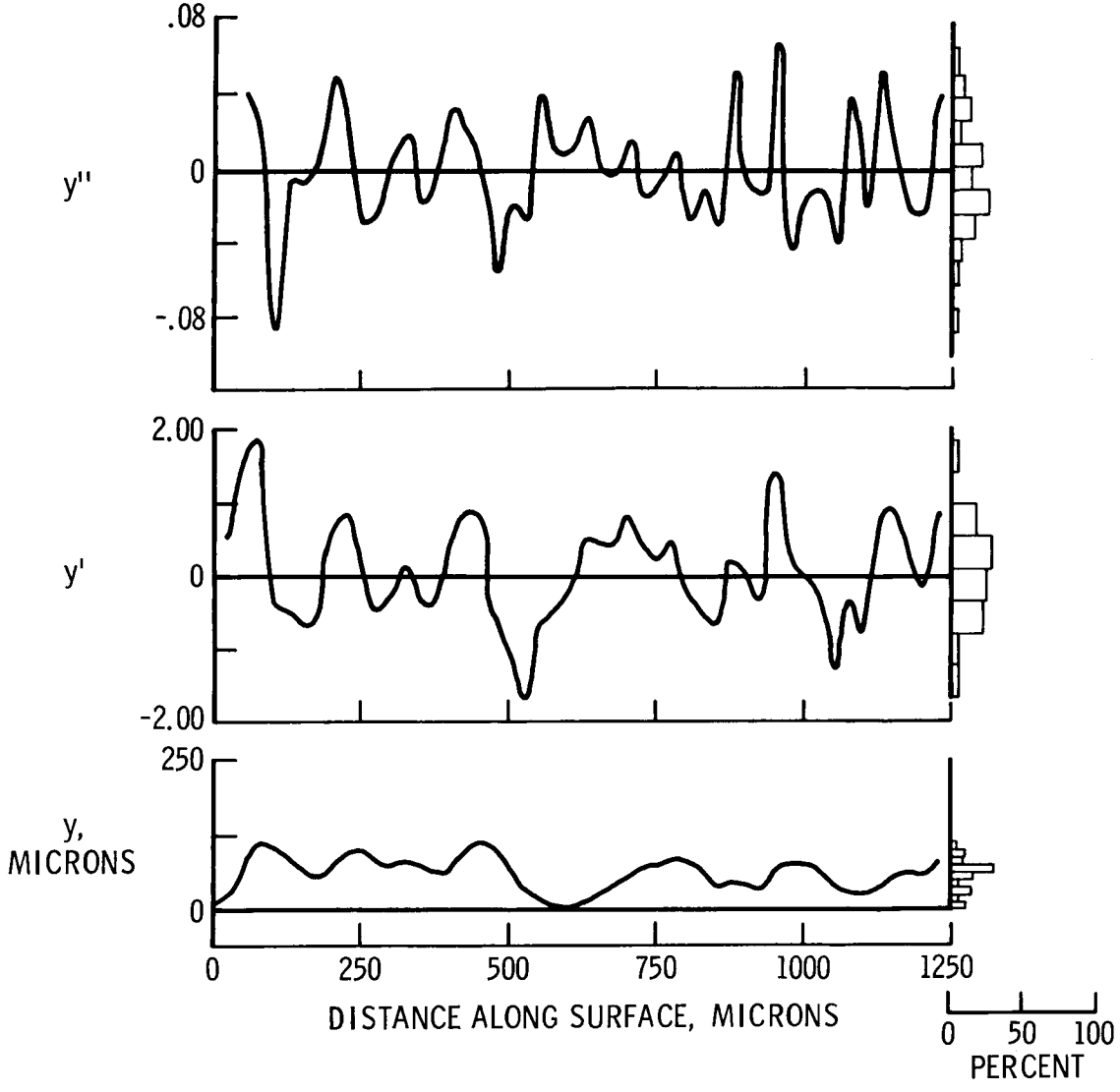

NASA

Figure 15.- Surface roughness of zirconia grit-blasted with No. 150F grit.

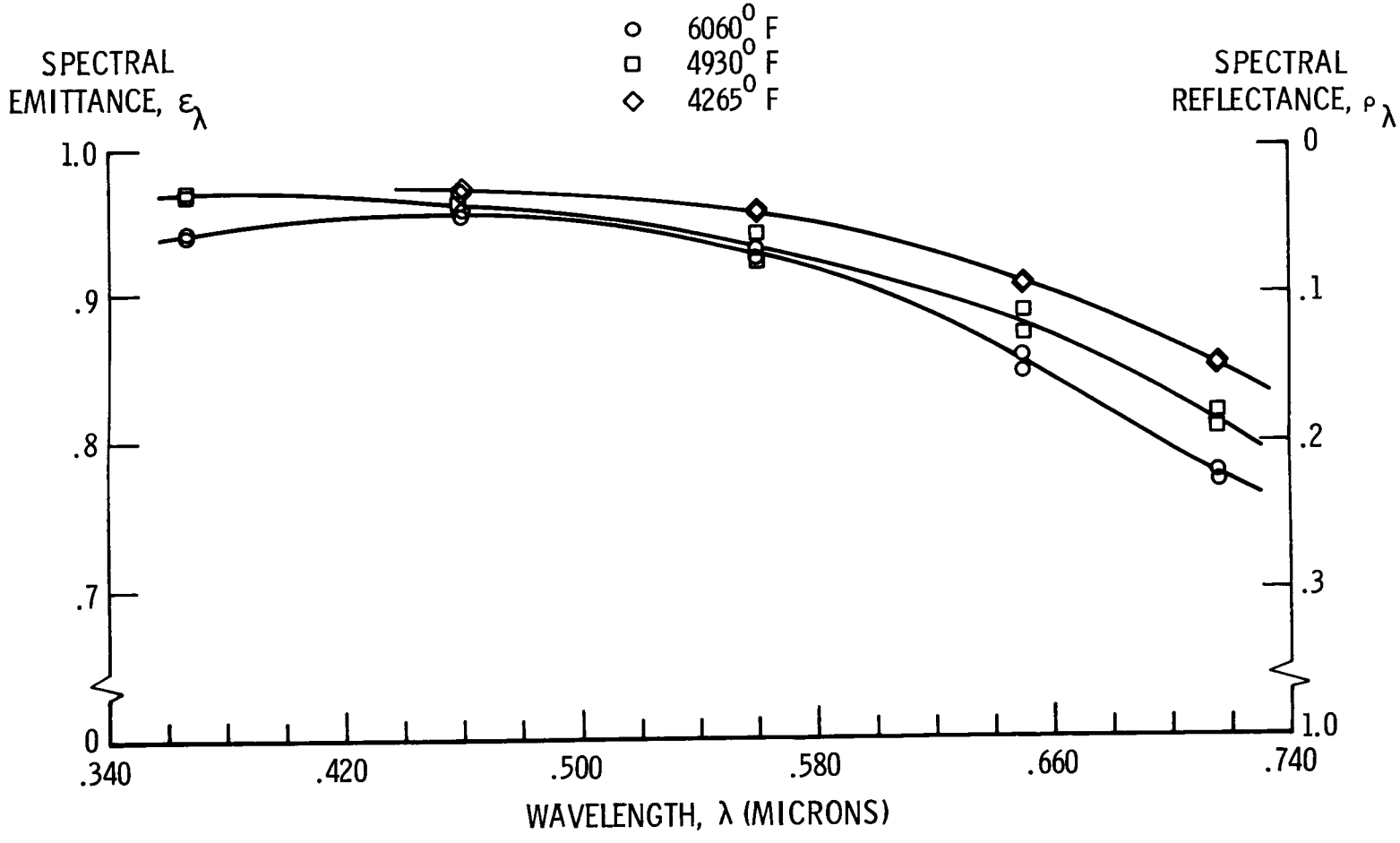

Figure 16.- Spectral emittance and reflectance of arc-jet-produced phenolic-nylon char versus wavelength.

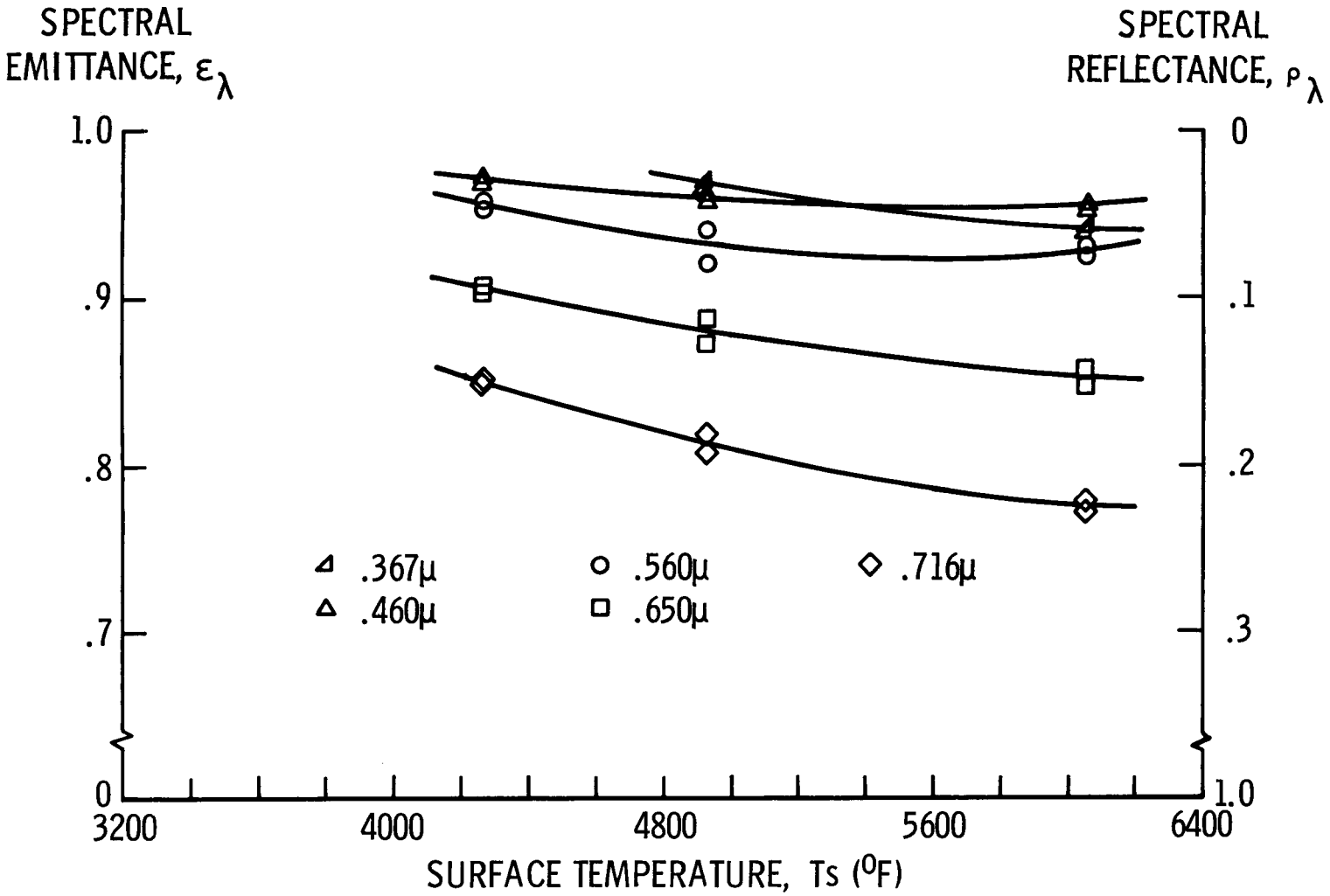

NASA

Figure 17.- Spectral emittance and reflectance of arc-jet-produced phenolic-nylon char versus temperature.

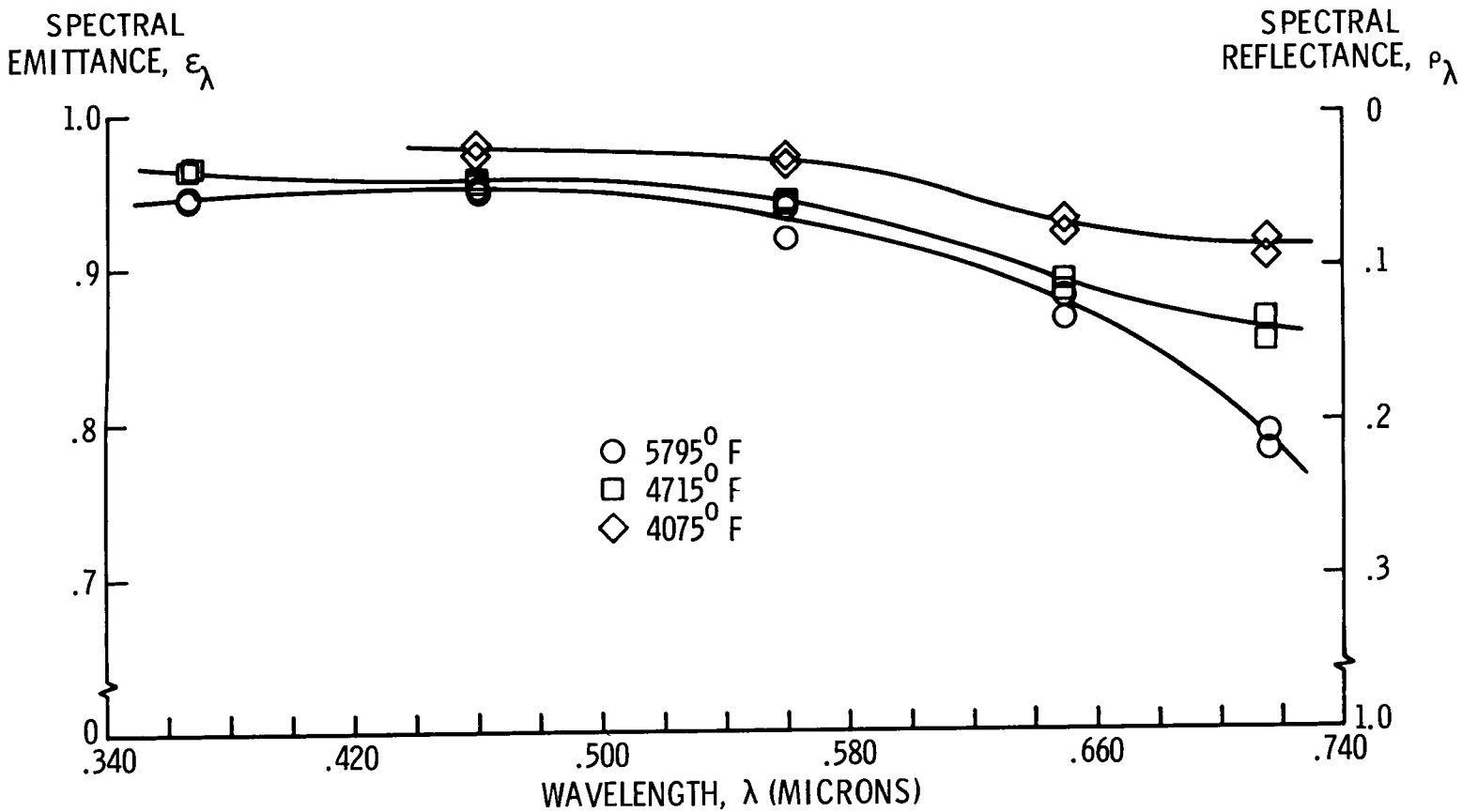

Figure 18.- Spectral emittance and reflectance of oven-produced phenolic-nylon char versus wavelength.

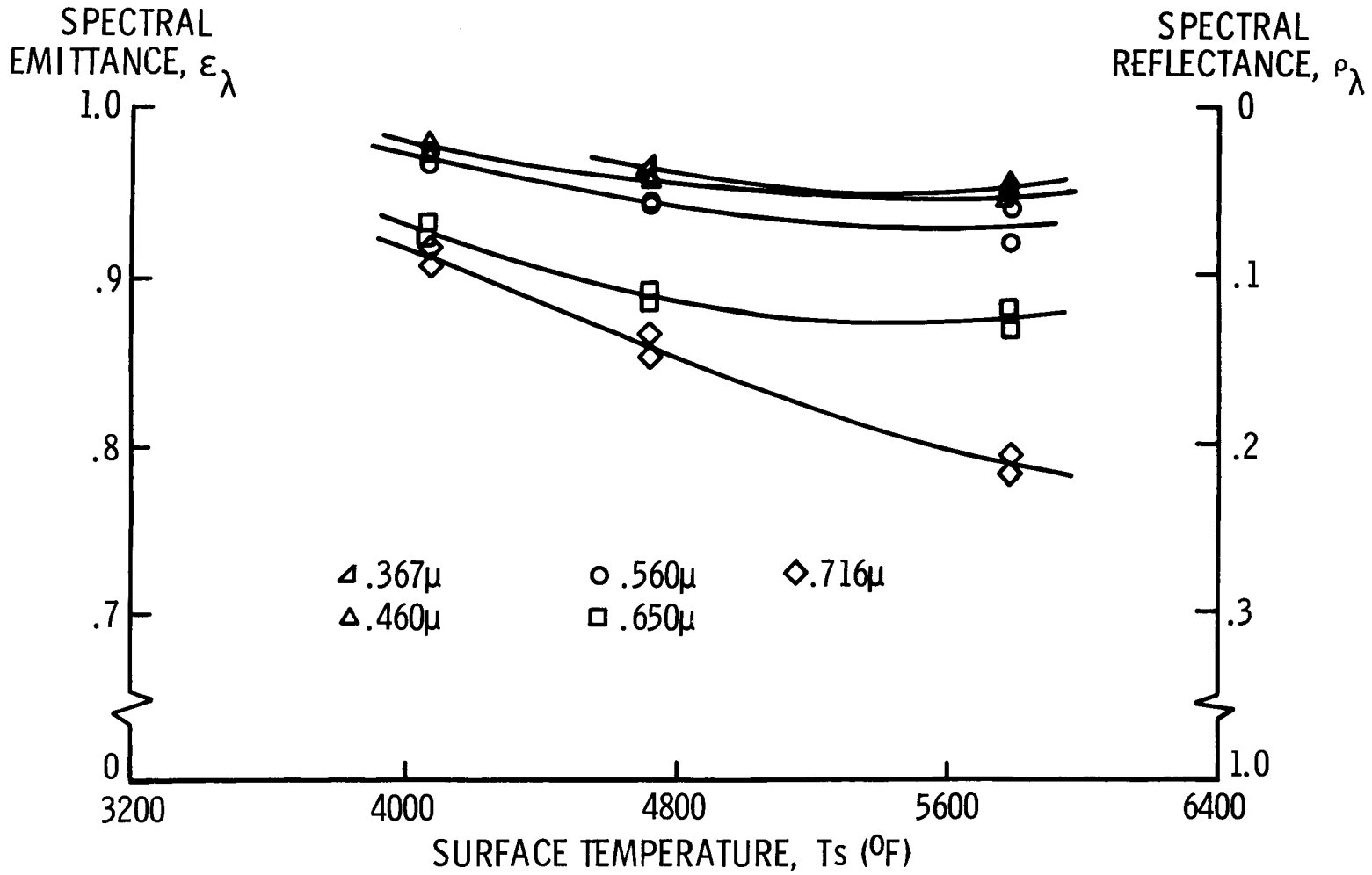

NASA

Figure 19.- Spectral emittance and reflectance of oven-produced phenolic-nylon char versus temperature.

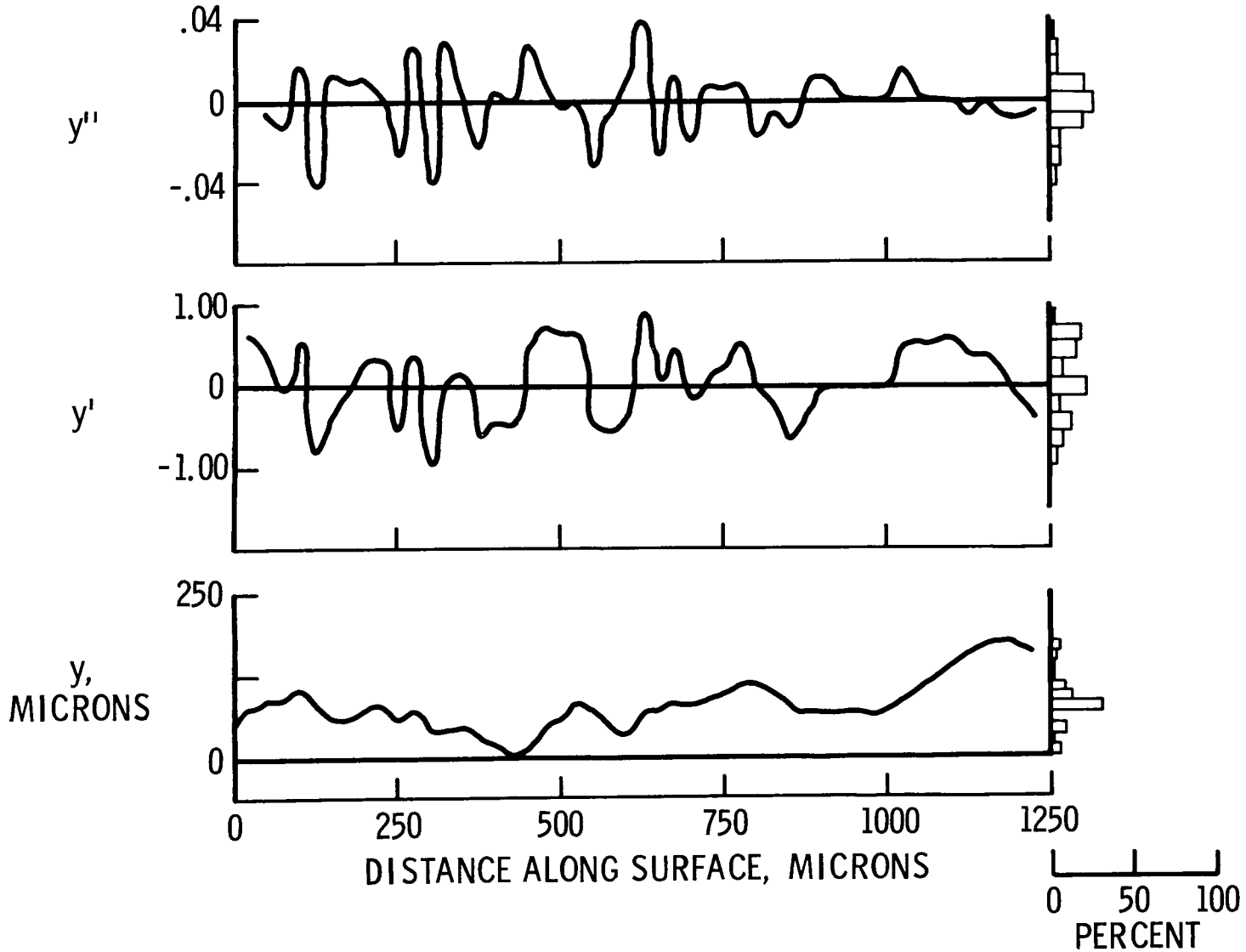

NASA

Figure 20.- Surface roughness of oven-produced phenolic-nylon char.

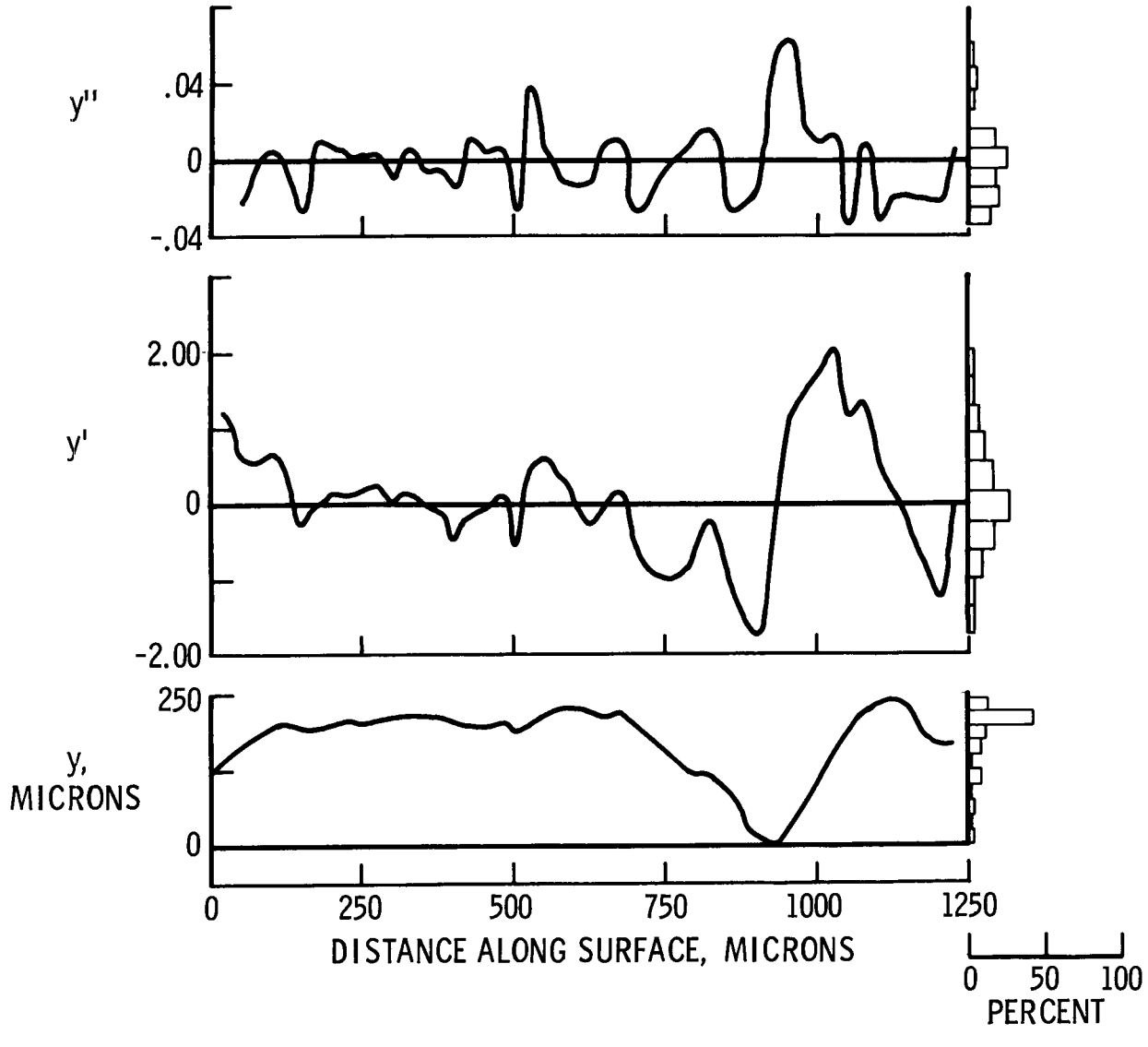

NASA

Figure 21.- Surface roughness of arc-jet-produced phenolic-nylon char.